BIOLOGICAL ROLE OF OSTEOACTIVIN , A PROTEIN

EXPRESSED BY TUMOR-CONDITIONED MACROPHAGES,

IN THE PROCESSES OF TUMOR GROWTH

AND TISSUE REPAIR

Relatore: Prof. Massimo Locati
Correlatore: Dott.sa Paola Allavena

Elaborato di: Manuela LIGUORI
Matricola: R10734

Anno Accademico 2016-2017

INDEX

ABSTRACT

Tumor-Associated Macrophages (TAM) are key orchestrators of the tumor microenvironment, directly affecting neoplastic cell growth, neo-angiogenesis, extracellular matrix remodeling and immunosuppression. In a gene profiling analysis on tumor-conditioned macrophages cultured *in vitro* with tumor cell supernatants, we identified a number of up-regulated genes. One of the most expressed gene was *Gpnmb*, coding for a protein called Human Glycoprotein non-metastatic melanoma protein B (*GPNMB*), also named Osteoactivin (OA). Osteoactivin is a trans-membrane and shed molecule with diverse biological functions, spanning from cell adhesion and migration, to immune-suppression and tissue repair. This study investigates the modulation of this protein and its functional role in monocytes/macrophages and TAM, in the tumor context. In human monocytes, expression of OA is up-regulated by anti-inflammatory stimuli, in particular IL-10, and corticosteroids. Immunostimulatory cytokines (IFNγ, IL-1β) or LPS are not stimulating its production. Accordingly, *in vitro* M2-polarized macrophages express more OA than M1-macrophages.

A spontaneous mutation of the *Gpnmb* gene occurred in the DBA/2J mouse strain. The mutation causes a premature stop codon and generation of a truncated non-functional protein. This strain, and the reconstituted DBA/2J-*Gpnmb*$^+$ mice with functional OA, are commercially available. OA-defective mice do not have obvious major problems, with the exception of the known rapid onset of glaucoma.

To clarify the role of this protein in the tumor microenvironment, we generated methylcolantrene-induced fibrosarcoma in these mice. Both mouse strains produced tumors with a similar incidence. We established and characterized 2 cell lines from DBA/2J*Gpnmb*$^+$ mice and 2 from DBA/2J mice. Tumors from DBA/2J mice grew earlier in DBA/2J*Gpnmb*$^+$ mice, indicating that the protein Osteoactivin produced by stromal cells, including TAM, enhanced tumor growth. To better understand the function of this protein, we generated isogenic cell lines expressing or not the functional OA protein (G2 OA and G2 MOCK cells). Osteoactivin -expressing cells grew faster

2

in vitro and under serum-free conditions were able to survive and to form spheroids which go on proliferating in an anchorage-independent manner. OA-expressing cells present typical cancer stem cell markers on their membranes such as Sca1, CD117 and SOX-2 and they are able to self-renew. The *in vivo* experiments demonstrated that Osteoactivin expression is associated with a significantly more aggressive phenotype, both in terms of tumor-take and tumor growth compared to OA-defective cell lines. We further demonstrated that OA-expressing tumors have higher mRNA levels of specific stem markers and in particular Nanog, SOX-2 and Brachyury.

From these data we can speculate that the production of Osteoactivin and its secretion by macrophages in the tumor microenvironment might be involved in the maintenance of cancer cell stemness and their proliferative potential.

INTRODUCTION

Macrophages: immunity and inflammation

The term "macrophage" comes from the Greek makros "large" and phagein "eat" and means "big eaters" and they were described for the first time in 1882 by Ilya Mechnikov [1].

Macrophages are large mononuclear cells (approximately 25-50 um diameter) with an irregular shape and they present membrane protrusions that help them in their activity of phagocytosis of pathogens or particulate matter. They constitute the mononuclear phagocyte system and represent the "first immune response" because they are the first cells of the innate immune system to enter inflamed tissues where they defend the body against pathogens. Macrophages display a great functional heterogeneity because, in addition to their role as "defenders", by secreting immuno-stimulatory cytokines to boost adaptive immunity, they are also very important during embryogenesis, development and tissue repair after damage. [2]

Macrophages originate from the hematopoietic stem cells which, under the influence of several cytokines such as IL-1, IL-6 and IL-3, give rise to the common myeloid progenitor granulocyte-monocyte colony-forming units (GM-CFU). From this common progenitor, through different steps of differentiation, are derived both neutrophils and both monocytes, the latter specifically driven by the growth factor Macrophage-Colony Stimulating Factor (M-CSF). However, recent evidence demonstrated that resident macrophages in peripheral tissues originate from hematopoietic precursors that were seeded during the embryonic development; few exceptions are the macrophages of specific sites such as the gastro-intestinal tract and the dermis [3, 4].

Monocytes express on their surface large amounts of the marker CD14 (a component of the receptor sensing bacterial lipopolysaccharide, LPS). Human peripheral blood monocytes also differentially express other antigenic markers which may be functionally related to their physiological activities. In fact we can identify "inflammatory monocytes" through the expression

of CCR2^{high}CD14^{high}CD16^{neg} and "patrolling monocytes" that are CX3CR1^{high}CD14^{dim}CD16^{pos}. In mice, monocyte subsets are defined by a set of slightly different markers: CCR2^{high}Ly6C^{high} and CX3CR1^{high}Ly6C^{low}, for inflammatory and patrolling monocytes, respectively. During an inflammatory response, the former monocyte subset is rapidly recruited at injured tissues and differentiates into macrophages, while patrolling monocytes are considered important to re-populate those peripheral tissues that are not dependent from embryonic precursors [3, 4].

In humans, in the peripheral circulation, mature monocytes constitute 5–10% of all blood leukocytes. The morphology of these cells can also be heterogeneous: they may have different size and degree of granularity and varied nuclear morphology [5, 6]

Pro-inflammatory, metabolic and immune stimuli all elicit increased recruitment of monocytes to peripheral sites, where differentiation into macrophages or DCs occurs, contributing to host defense, tissue remodeling and repair. This process is strongly mediated by chemokines and chemokine receptors (for example CCL2 and its receptor CCR2, CX3CL1 and CX3CR1) that allow adhesion to endothelial cells and tissue entry [7, 8]

The development of macrophages from monocytes is regulated by growth factors among which the most important is M-CSF, also called Colony Stimulating Factor (CSF1), guiding their differentiation as well as their proliferation and viability. A combination of different markers expressed on cell surface, such as CD68, CD14, CD16, CD11b and CD163 allows the identification of differentiated macrophages. However, it has become increasingly clear that, depending on the local stimuli, macrophages could be activated in various ways, with profound changes in gene expression profiles [5, 6, 9].

The current shared view about macrophage polarization considers dividing them in at least two general classes based on their phenotype and function: M1 (classically activated) and M2 (alternatively activated). M1 macrophages are generated from monocytes stimulated with LPS and IFNγ; once differentiated they produce high levels of IL-12 , IL-1, IL- 23, TNFα and CXCL10, playing a fundamental role in the development of inflammatory processes: they have high microbicidal activity, immuno-stimulatory functions and are cytotoxic for tumor cells. These

macrophages can be identified from their surface antigens MHC II, CD80 and CD86 that are up-regulated during M1 polarization [7, 10-12].

On the other hand, M2 macrophages are critical effectors in parasitic infections and fundamentally contribute to tissue healing after injury by scavenging of debris, tissue remodeling, angiogenesis and resolution of inflammatory processes. They originate from monocytes differentiated in the presence of IL - 4, IL- 13, IL-10 or corticosteroids and, once mature, are able to secrete IL- 10, CCL17, CCL22, CCL18 and IL- 1ra. The M2 polarization is characterized by the over-expression of CD206 (mannose receptor-1) on cell membrane, CD163 and other scavenger receptors [11].

The loss of equilibrium of both M1 and M2 cell number may lead to pathological events: an M1 excess could be the cause of chronic inflammatory diseases whereas an uncontrolled number of M2 could promote immune suppression. [11, 13].

However, due to the high heterogeneity of macrophages, it is now considered that the M1- and M2-polarization is an over-simplification and just constitutes the two extremes of a wide panel of distinct phenotypes and functional states of the macrophages. Indeed, stimuli available in different pathological conditions, such as acute versus chronic inflammation, infection and cancer, activate distinct functional responses characterized by distinct transcriptional programs [12, 14, 15].

Macrophages in tumors

Macrophages are a numerically abundant population in tumor tissues and it is now established that they contribute to the reactive environment, characterized by a low grade cancer-related inflammation [16-18]

Macrophages in tumors derive from circulating monocytes, which are herein recruited by chemotactic factors, among which one of the most important is the chemokine CCL2 originally named Monocyte Chemotactic Protein 1(MCP-1) [19-21].

In tumors, CCL2 can be produced by macrophages themselves as well as by stromal and cancer cells. Other important factors are the chemokines CCL5, CCL7, CXCL8 and CXCL12; the Vascular Endothelial Growth Factor (VEGF), Platelet Derived Growth Factor (PDGF), M-CSF, but also fibronectin, fibrinogen and other factors produced during the cleavage of extra-cellular matrix (ECM) proteins elicited by macrophage- and/or tumor cell-derived proteases [11].

When blood monocytes migrate into tumor tissues they differentiate in Tumor-Associated Macrophages (TAM). TAM could represent up to 50% of the tumor mass, and operate as fundamental actors in the cross-talk between neoplastic and immune cells. There is now a general consensus that high TAM density in tumors is associated with faster disease progression and negative patient prognosis in several human neoplasms for example in lymphomas and in pancreas, breast and lung cancers. [6, 22-25]

Within tumors, macrophages are in contact with different signals such as M-CSF that induces their differentiation, and other molecules that inhibit the M1 polarization, such as IL - 10 and TGFβ. Indeed, several studies have shown that TAM have similar characteristics as M2 polarized macrophages because they do not secrete high levels of inflammatory mediators, have pro-angiogenic and immunosuppressive activity. [13]. However, the complexity of the tumor microenvironment and the low-grade inflammation often associated with cancer can induce more

nuanced or mixed phenotypes in TAMs, which show both inflammatory/anti-inflammatory and immunosuppressive characteristics [26].

Within the tumor microenvironment, macrophages can affect different fundamental aspects of the neoplastic population. For instance they promote tumor cell proliferation, via the production of growth factors (e.g. Epidermal Growth Factor, EGF); they support the mobility of cancer cells, favoring their invasion of surrounding tissues and distant metastatization. TAM accumulate in hypoxic areas within the tumor, where they stimulate angiogenesis by expressing several pro-angiogenic factors and recruitment of other hematopoietic cells. Furthermore, TAM contribute to the buildup of the stromal matrix architecture by producing important components, including glycoproteins: osteopontin, fibronectin; proteoglycans: SPARC, different collagen types and proteolytic enzymes. In collaboration with neoplastic cells, they can also influence fibroblasts by producing growth factors such as EGF, FGF, PDGF and, above all, TGFβ. In turn, activated fibroblasts release other biologically active mediators for epithelial cells (IGF, EGF, HGF), or macrophages (CCL2, CXCL12).
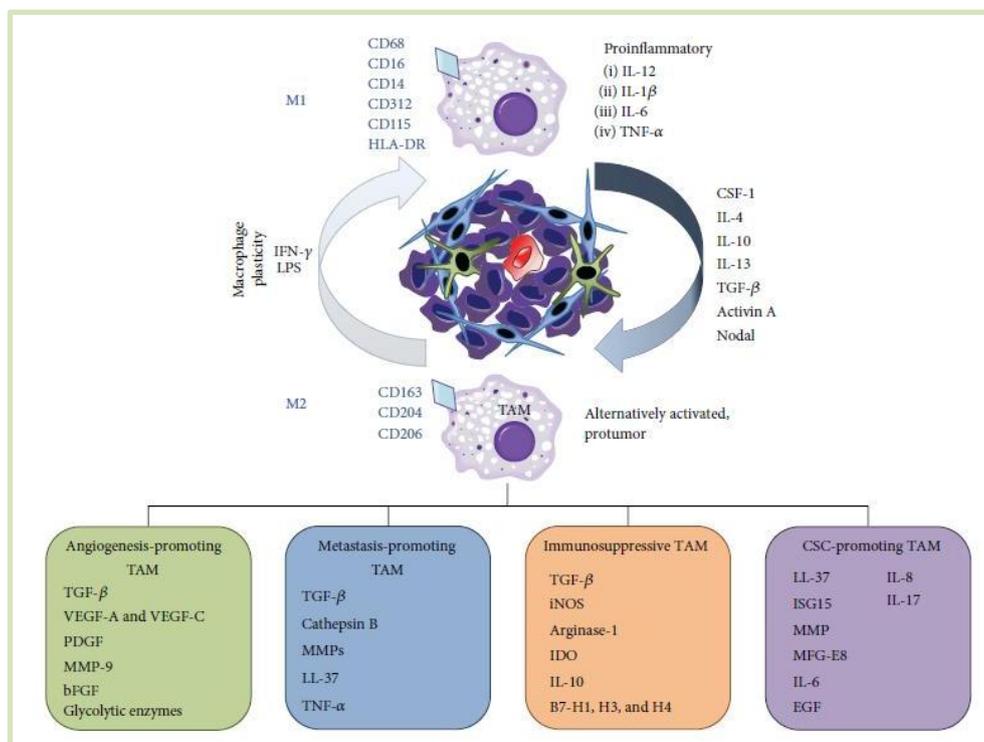

Fig 1. **Macrophage plasticity and TAM characterization**. TAM functions are multiple and they include angiogenesis, metastatization, immunosuppression and support for cancer stem cell function. [27]

The tumor microenvironment

Solid tumors are composed by two different compartments: the parenchyma and the stroma that are often undistinguishable to each other [28, 29]. The parenchyma is made by cancer cells while the stroma includes various non-malignant cells types including fibroblasts, blood vessels and immune cells. In the tumor microenvironment (TME) we can recognize:

-Resident components: cells and structural factors that are stably present within the milieu of the stroma.

-Non-resident components: immune cell populations that infiltrate the neoplastic microenvironment by extravasation through blood vessels; their recruitment is controlled by chemokines and factors produced by resident components.

Various molecules are produced by these cells that are secreted into the extracellular space creating a very intricate network that support and sustain important activities of the tumor itself. This matrix is called extracellular matrix (ECM).
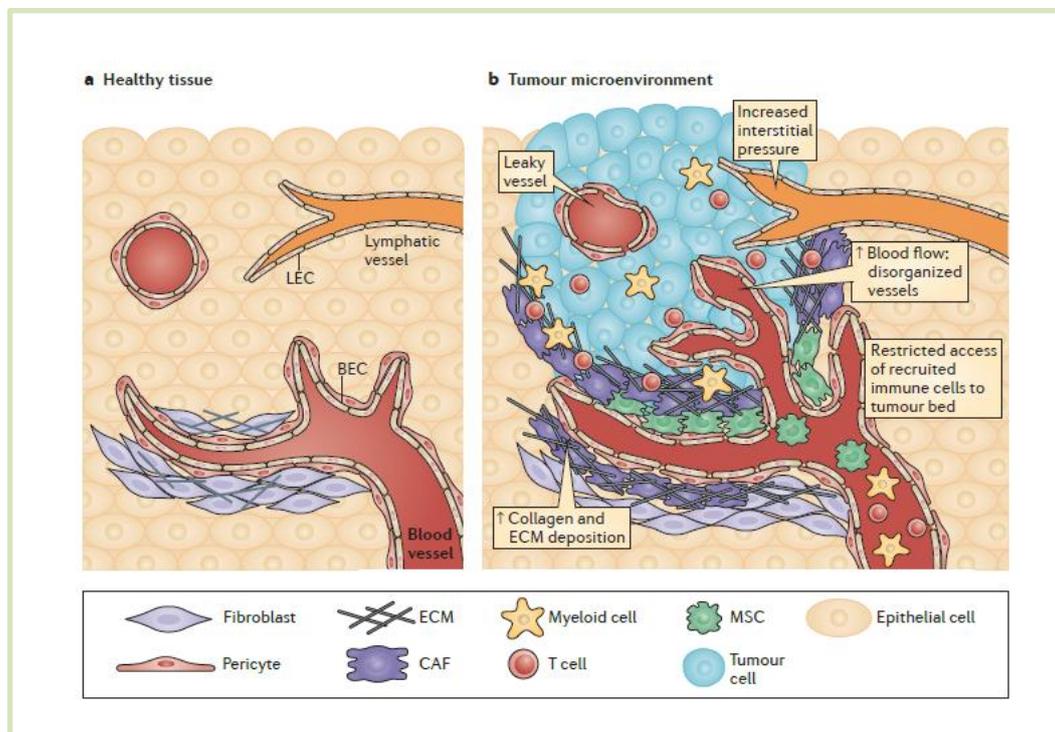

Fig 2. **Composition of tumor microenvironment.** In addition to cells and structural factors stably present within the milieu of the stroma into tumor microenvironment we can find different cell populations such as MSC, myeloid cells, fibroblasts and various protein belonging to the extracellular matrix [30].

The extracellular matrix

The ECM is composed of a large collection of biochemically distinct elements including proteins, glycoproteins, proteoglycans and polysaccharides, with different physical and biochemical properties. All ECM elements appear aggregated to each other and to the surface of cells that produce them, in an organized compact network. In the past it was thought that the ECM could serve as an inert scaffolding able to stabilize tissue structure, but it is now universally recognized that the ECM is functionally relevant and able to support cell adherence, migration, proliferation and differentiation, also influencing cell survival, shape and function [31]. The interaction between cells and extracellular matrix as well as composition/remodeling of ECM itself, can control physiological phenomena such as morphogenesis, pathophysiological events as wound healing, and pathological processes, like tumor invasion and metastatization [32, 33].
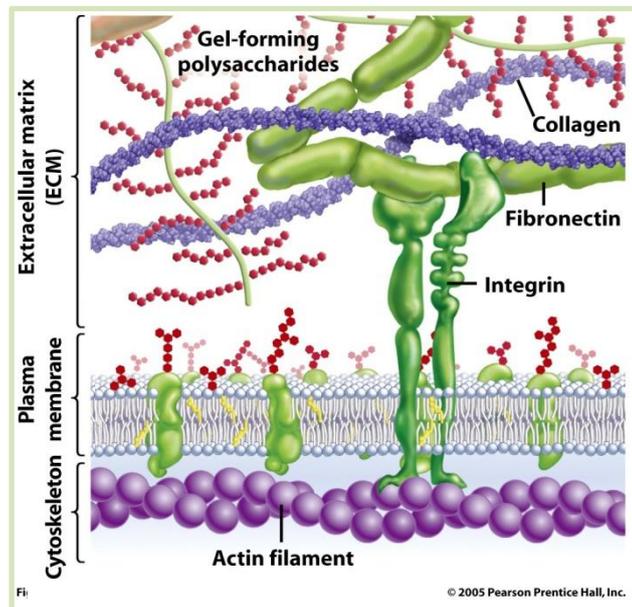

Fig 3. Composition of the extracellular matrix. Collagen, fibronectin, polysaccharides are organized in a compact network.

The correct homeostasis between ECM deposition and degradation (matrix remodeling) is a complex and tightly regulated physiological process. Alteration in this homeostasis is relevant for a number of pathological events. For example, excess of ECM production or reduced ECM turnover are prominent in tissue fibrosis of many organs like pulmonary and renal fibrosis, systemic sclerosis, liver cirrhosis and cardiovascular disease. [34, 35]. Abnormal ECM dynamics are well documented also during tumorigenesis and metastatic progression of cancer. Various collagens, including collagen I, II, III, V, and IX, show increased deposition during tumor formation [36, 37], and increased MMP activity [38]. Moreover, many ECM components and their receptors, such as heparan sulfate proteoglycans and CD44, facilitate growth factor signaling and are frequently overproduced in cancer [39-41].

The intense protease activation and ECM turnover in inflamed tissues are affected by cytokines, such as TGFβ, TNFα and IFNγ that are produced by inflammatory cells. Infiltrating immune cells release cytokines and proteases (e.g. MMPs) that in turn activate resident fibroblasts cells. This leads to an aberrant synthesis and/or cleavage of ECM components, contributing to the perpetuation of the inflammatory response towards the development of chronic inflammation [42].

ECM has an important role in influencing immune cell behaviour during the inflammatory process: the individual elements of the ECM and its three-dimensional structure can signal specific information to cells and modulate immune cell migration into and within inflamed tissues, immune cell activation and proliferation, and cell differentiation processes, such as T cell polarization [43].

ECM remodeling in the tumor microenvironment

All tumors are characterized by their own heterogeneous and very dynamic microenvironment that evolves gradually along tumor growth, as a result of the tumor-host interaction.

All the components of tumor microenvironment: cancer cells, non-cancer cells (endothelial cells, tumor-associated fibroblasts and immune cells, including macrophages), soluble factors (growth factors, cytokines, chemokines and proteolytic enzymes) take part in the intense remodeling and modification of the matrix that generates a microenvironment more and more suitable for tumor growth and progression. Nevertheless, macrophages within tumors are by far the main actors responsible for the constant transformation of the tumor microenvironment [44].

Macrophages work through two important processes:

1) The degradation of molecules present in the ECM activated or induced by neoplastic cells through specific proteases which can be grouped in large families and include matrix metalloproteases (MMPs), cathepsins, hyaluronidases, ADAM proteases, but also heparanase, elastase, urokinase-type plasminogen activator (uPA), plasmin and others, induced by neoplastic cells [45];

 2) The synthesis of new components of the ECM [46, 47];

ECM molecules have the ability to interact with cell surface receptors and with biological mediators such as cytokines, chemokines, growth factors and proteases. These interactions may profoundly affect cellular functions both on the tumor side as well as on the side of stromal, vascular and immune cells. Among the most important and mostly studied ECM molecules are: fibronectin, thrombospondin, osteopontin, collagens and SPARC (secreted protein acidic and rich in cysteine).

Fibronectin (FN): is involved in many cellular processes, including cell migration and adhesion, tissue repair, blood clotting and embryogenesis. FN exists in two main forms: an insoluble glycoprotein in the ECM (extracellular matrix) and a soluble one present in the plasma. The ECM form is produced by fibroblasts, macrophages, endothelial and epithelial cells; here FN organizes

interactions between various matrix components (proteoglycans) and different cells, via binding to specific integrin receptors [48].

Thrombospondins: are a family of secreted ECM proteins produced by several cell types in response to injury and during tissue remodeling; the thrombospondin family includes five members TSP-1, TSP-2, TSP-3, TSP-4, and TSP-5 [49].

Osteopontin: is a component of the ECM produced by stromal and tumor cells. In the tumor microenvironment osteoponting is involved in protease activation and ECM remodeling, cell adhesion and migration, angiogenesis, as well as in inflammation and immunity [50, 51].

Collagens: are major components of the ECM and they represent about 30% of the total protein mass in the body. There are 28 different types of collagens which exist in fibrillar and non-fibrillar forms. Collagens can act as a scaffold, facilitating migration of invading cancer or stromal cells into ECM.

SPARC (secreted protein acidic and rich in cysteine, also known as osteonectin): is a protein with the ability to bind to several resident components of the ECM such as thrombospondin 1, vitronectin, entactin/nidogen, fibrillar collagens (types I, II, III, and V), and collagen type IV, modulating growth factor efficacy, affecting the expression of matrix metalloproteinases with an important contribute to the organization of ECM itself [52].

The inflammatory tumor microenvironment:

Cancer associated inflammation is now recognized as a hallmark of tumors[17]. Macrophages associated to the tumor microenvironment are the major source of inflammatory mediators, though a number of inflammatory cytokines can be produces also by cancer cells [16, 53].

As mentioned before, the interaction between neoplastic and immune cells is fundamental in the processes of tumorigenesis, tumor growth and metastasis. These processes are directly influenced by many growth factors and by pro-inflammatory as well as anti-inflammatory cytokines. These soluble or matrix-bound mediators constitute a very intricate network that allows the cross-talk between tumor, immunity and stromal cells[54].

IL-6 is a pro-inflammatory cytokines that contributes to angiogenesis, promotes B and T cell differentiation and stimulates tumor cell proliferation [55]. Other pro-inflammatory factors derived from macrophages or other immune cells include IL-1β, TNFα and IFN-γ.

Transforming growth factor beta (TGFβ) is a "double action" factor with both pro and anti-tumorigenic activities; TGFβ can suppress growth or inhibit cancer progression activating the apoptosis process. It is also a strong inducer of the epithelial-to-mesenchymal cell transition (EMT), which can induce de-differentiation of cancer cells which acquire cancer stem-cell-like phenotype and motile phenotype. TGFβ is also a potent immune-suppressive factor [56].

Other inflammatory mediators include IL-10, a potent immunosuppressive factor that inhibits T cell-mediated tumor destruction and vascular endothelial growth factor (VEGF) which supports angiogenesis and inhibits DC function and migration. Malignant transformation is often associated with aberrant production of FGF (fibroblast growth factor) and EGF (epidermal growth factor) which stimulate angiogenesis and proliferation of both tumor and stromal cells. [57, 58].

Tumor-conditioned macrophages

Our group previously set up an *in vitro* model of co-culture between cancer cells and human monocytes, and selected those cell lines able to induce the differentiation of monocytes into macrophages. We next demonstrated that the cell lines with this biological activity were producing the growth and differentiation factor M-CSF, beyond other biological mediators. The phenotype and functional activity of these Tumor-Conditioned Macrophages (TC-Macro) differed from classically activated M1 macrophages and these cells were indeed more similar to M2 macrophages. An Affymetrix gene profiling analysis of TC-Macro and by comparison of TAM isolated from human ovarian carcinoma revealed that indeed the TC-Macro are very similar to ex vivo human TAM, supporting the validity of our *in vitro* co-culture system [59]. Considering the gene expression analysis of TC-Macro, we found that among the most up-regulated genes were several genes coding for ECM proteins or related to its remodeling. Among proteolytic enzymes, the most expressed were MMPs (12, 9, 1 and 14), Cathepsins (L, C, Z and B), uPA, lysosomal enzymes and ADAM proteases.
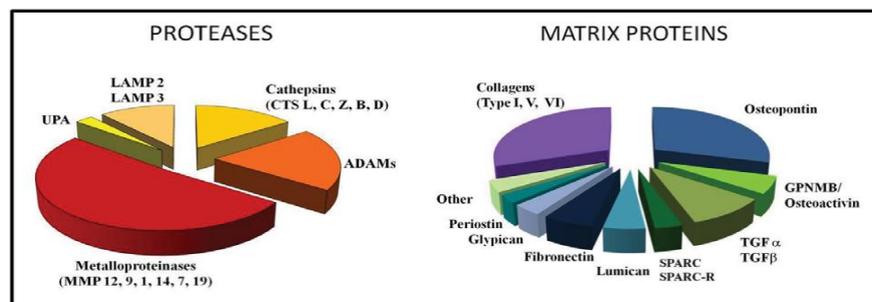
Fig 4. Gene profiling of human TAM. The scheme shows the expression of genes coding for ECM proteins end proteolytic enzymes implicated in its degradation/remodeling [47].

Regarding matrix proteins we observed that Collagens, Osteopontin, *GPNMB* and Fibronectin were the most overexpressed genes. In particular we decided to focus our studies on *GPNMB* [59].

Glycoprotein non - metastatic melanoma protein B (*GPNMB*) is a highly glycosylated type I transmembrane protein also named Osteoactivin (OA). It was first described in 1995 as a protein

that shares significant sequence homology to melanosomal proteins: with the human protein and murine nmb (Non- metastatic melanomal protein B), with the protein PMEL 17, dendritic cell-associated heparin sulfate proteoglycanintegrin ligand (DC-HIL) or hematopoietic growth factor inducible neurokinin-1 type (HGFIN) [60].

The *Gpnmb* gene is localized to human chromosome 7 and mapped to mouse chromosome 6. The highly conserved *Gpnmb* gene consists of 11 exons with an open reading frame of 1716 bp and encodes for a protein of 572 amino acids. The protein consists of an extracellular domain (ECD) that contains a signal peptide and a cleavage site at position 23 as well as a polycystic kidney disease (PKD) domain, 13 predicted N-linked glycosylation sites and an Arg-Gly-Asp (RGD) motif as integrin-binding site at position 556 and a cytoplasmic domain of *GPNMB*, called Osteoactivin , with a conserved di-leucin-based endosomal/melanosomal-sorting signal [60, 61].

Osteoactivin has two isoforms, a transmembrane type I 65k -Da isoform and a highly glycosylated secreted isoform 115k –Da. Osteoactivin   is expressed in a wide variety of human and mouse tissues and cell types such as melanocytes, endothelial cells as well as dendritic cells and macrophages . Within cells it is localized to the cell surface as well as into vesicular, endosomal- or lysosomal-like structures. The secreted form is released by cells via ectodomain shedding. This process is regulated by protein kinase C as well as intracellular $Ca2^+$-dependent pathways and it is mediated by MMPs and a disintegrin and metalloproteinase ADAM10 [62]. The cleaved form of Osteoactivin , which possesses the heparin-binding RGD motif, actually binds to a heparin sulfate proteoglycan-type receptor similar to the FGF receptor. It was furthermore shown that Osteoactivin on the surface of dendritic cells can bind to endothelial cells via its RGD motif as well as to T cells via the PKD domain [63]. The interaction between dendritic cells and T cells is actually mediated by the binding of Osteoactivin to syndecan-4 on T cells, which in turn leads to an inhibition of T cell responses[64]. In macrophages, the glycoprotein is present in the Golgi apparatus and was shown to be over-expressed following interferon (IFN)-γ or lipopolysaccharide (LPS) treatment [65].

The expression of Osteoactivin in osteoblasts and melanocytes was shown to be regulated by the microphthalmia transcription factor (MITF) via a MITF-binding site (M-box) that is present in the *Gpnmb* promoter [66, 67]. In skeletal muscle cells after denervation, basic fibroblast growth factor (bFGF) and platelet-derived growth factor (PDGF) have been shown to regulate the expression of Osteoactivin [68].

To identify the biological functions of this protein has been challenging, both for the great variety of biological processes in which it appears to be involved, and for the contrasting results published in the literature.

Osteoactivin plays an important role both in physiological and pathological conditions. In fact it seems to have an important role in fibroblast differentiation, in the maintenance of bone homeostasis and in particular during growth and differentiation of osteoblasts / osteoclasts [69]. Osteoactivin is furthermore essential for normal eye function: the protein is highly expressed in retinal pigment epithelium and iris during embryonic development. Studies using DBA/2J mice, which spontaneously underwent a premature stop codon mutation in the *Gpnmb* gene (*GPNMB*R150X), it has been demonstrated that these mice have pigment dispersing iris disease and subsequent age-related pigmentary glaucoma. The absence of Osteoactivin mediates a melanosomal defect associated with cellular debris shedding in the eye chamber which consequent inflammation of the iris, atrophy and finally glaucoma [70, 71].

Osteoactivin is up-regulated in several types of cancer. It was described for the first time in low-metastatic human melanoma cell lines, but subsequent studies suggested that this protein is expressed by highly malignant tumors and promotes invasion and metastasis (with a correlation with over-expression of MMP-2/9 and MMP-3). Several studies also reported a high expression of Osteoactivin in cutaneous melanomas, in aggressive human breast cancers and other malignant tumors where it is able to induce cancer metastasis to bone [72, 73].

In addition, a number of studies demonstrated a pathophysiological role of Osteoactivin in various disease models associated with inflammation and fibrosis. In skeletal muscle affected by denervation, Osteoactivin was found to be up-regulated in myofibers and this might correlates with

17

an hypothetical role in ECM regeneration and fibrosis. Osteoactivin can interact with infiltrated fibroblasts, which in turn stimulates the expression of MMP-3, MMP 9 and collagen I [74]. Another study by the same group demonstrated that the overexpression of the protein protects skeletal muscle from severe degeneration caused by long-term denervation in mice, accompanied by decreased infiltration of fibroblast-like cells, up-regulation of anti-fibrotic genes and lower levels of collagen deposition. In addition, the Osteoactivin ectodomain shedding induces MMP-3 expression in mouse fibroblasts through the activation of the ERK pathway. The activation of ERK1/2 and p38 in the MAPK pathway may be involved in the attenuation of fibrosis [74]. In kidney, the protein was found to be strongly induced in tubular endothelium and interstitial fibroblasts after unilateral ureteral obstruction in rats with probable implication in regenerative processes and fibrosis upon injury. Moreover in monocytes and macrophages of mice after ischemic kidney disease there is an overexpression of Osteoactivin which suggests the protein as a novel biomarker of progressive kidney disease using DBA/2J mice, Li and colleagues revealed that the absence of functional Osteoactivin results in impaired phagocytosis and autophagy responsible for the degradation of internal debris and apoptotic cells [75]. This event led to higher mortality rates of these mice associated with increased apoptosis rates and prevention of normal organ repair. These results suggest that Osteoactivin is involved in the repair after kidney damage by affecting macrophage function. All these results indicate that this protein plays an important role in inflammation, during fibrosis after injury in skeletal muscle, liver and kidney [65, 68, 76-78].

The evidence that the *Gpnmb* gene coding for the protein Osteoactivin was highly upregulated in tumor-conditioned macrophages (*in vitro* co-culture system of tumor cells and macrophages), prompted us to investigate the biological significance of this upregulation, especially in the connection between Tumor-Associated Macrophages and cancer cells.

Aim of this study is to understand the biological role of Osteoactivin produced by macrophages, in the context of the pro-tumor functions of these immune cells.

In particular, we focused our attention on the regulation of this protein both in human and mouse phagocytic cells and on its biological role in the tumor microenvironment.

For the *in vivo* study we took advantage of the mouse strain DBA/2J with a spontaneous non-functional mutation in the *Gpnmb* gene. The Jackson Company generated a transgenic mouse line reconstituted with the native functional protein: DBA/2J-*Gpnmb*$^+$ mice. Therefore, both mice with non-functional Osteoactivin and mice with the functional protein were available for this study and greatly helped in the understanding of the biological function of Osteoactivin in experimental tumor models.

Production and regulation of Osteoactivin in monocytes/macrophages:

We previously demonstrated that *Gpnmb* is strongly upregulated (>85 fold) in tumor-conditioned macrophages (TC-Macrophages), cultured with tumor cell supernatants [59].

In Fig 5 are summarized the results of the transcriptional profile analysis from our AffyData database. RNA was extract from monocytes freshly isolated from 3 different donors (Mono) and from in vitro M-CSF-differentiated macrophages (M0), further polarized to M1 and M2 cells; *Gpnmb* expression was very low in all monocytes analyzed (grey columns) while was greatly increased in their respective M0 and M2 polarized macrophages (orange and purple columns respectively). Of note, M1 macrophages (pink coumns) had lower expression (Fig.5A).

We also investigated Tumor-Associated Macrophages (TAM) isolated and purified from human ovarian carcinoma (green columns). *Gpnmb* mRNA levels were considerably elevated in human TAM (Fig.5B). These results confirm our original observation obtained with TC-Macrophages exposed *in vitro* to tumor cell supernatants (light blue columns) where *Gpnmb* is highly upregulated compared to monocytes cultured alone (Fig.5B).
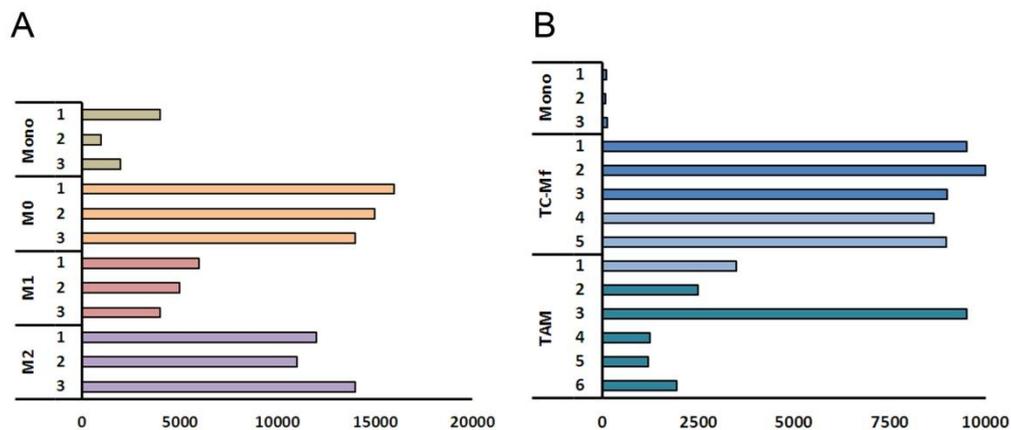
Fig 5. Transcriptional profile analysis of the *Gpnmb* gene in different human macrophage populations. A) Monocytes were freshly isolated from buffy coats and macrophages differentiated from monocytes using M-CSF for 6 days (M0) and polarized with LPS and IFNγ (M1) or IL-4 (M2) for 24 hr. B) TC-Macrophages were cultured for 72 hrs with tumor supernatants from the pancreatic cell lines PANC1 or ASPC1; TAM were isolated from human ovarian carcinoma. Data are shown as hybridization signals from the Affymetrix chips.

In order to gain insights into the functional role of Osteoactivin expression in monocytes/macrophages, especially in the tumor context, the first purpose of the thesis was to study the regulation of Osteoactivin production in myeloid cells.

For this purpose we evaluated Osteoactivin protein expression in human and murine monocytes and macrophages in response to different stimuli and in the presence of distinct tumor cell supernatants. The transmembrane isoform of Osteoactivin was investigated by flow cytometry with a commercial anti-Osteoactivin mAb. In human monocytes, Osteoactivin expression was upregulated by the anti-inflammatory cytokine IL-10 and by glucocorticoids, but not by immuno-stimulatory cytokines, such as IFNγ, or LPS, which actually repressed its expression (Fig 6).
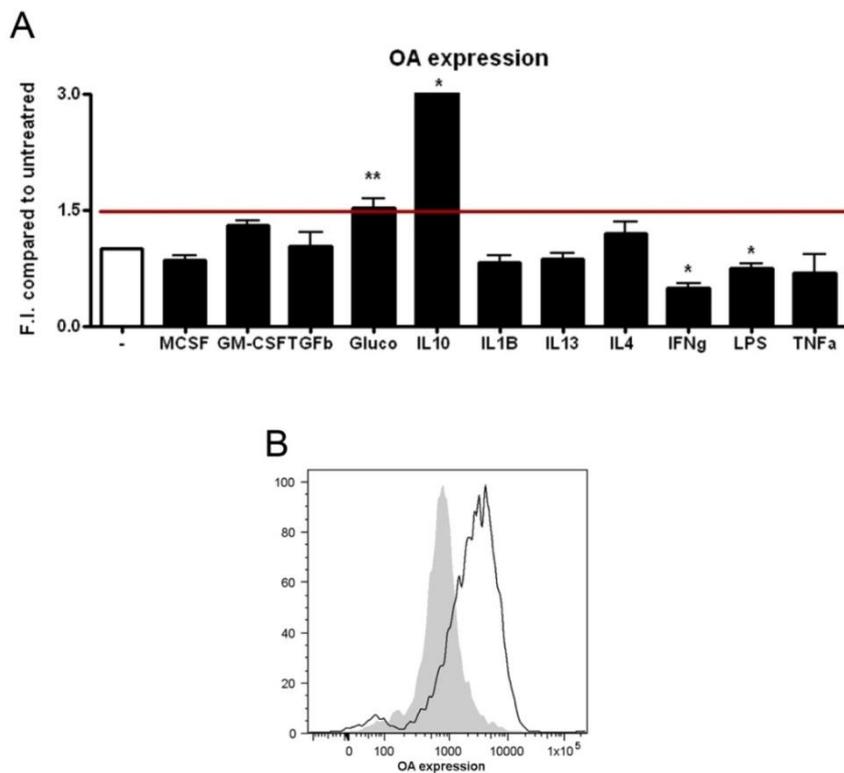
Fig 6. Modulation of the transmembrane isoform of OA in human monocytes. A) Flow cytometry analysis of the transmembrane form of OA in human monocytes treated with different stimuli for 24 hr. OA is up-regulated by anti-inflammatory stimuli (IL-10, glucocorticoids) and not by pro-inflammatory ones. Data are shown as fold increase over untreated monocytes (-), (mean -/+ SD of 3 exp); the red line indicates the level beyond which our data are considered significant (1,5 F.I.). Statistical analysis: *p < 0.05, **p < 0.01, (Student's t test). B) Representative phenotype profile of OA expression in glucocorticoids-treated monocytes (24h). The grey profile represents the control untreated cells; the black line represents the expression of Osteoactivin in stimulated monocytes.

21

We next studied the soluble isoform by ELISA in TC-Macrophages and in polarized M1 and M2 macrophages. To generate tumor supernatants we used four different pancreatic tumor cell lines (PT45, PANC1, ASPC1 and MIaPaCa), an immortalized non-tumorigenic pancreatic cell line (HPDE) and an ovarian carcinoma cell line (K-ov). Human macrophages released Osteoactivin in response to supernatants from PT45 and PANC1 cells but not when exposed to the other cell lines (Fig. 7A) , Of note, none of these cell lines constitutively produced this protein (data not shown). Osteoactivin release from *in vitro* differentiated and polarized macrophages, surprisingly showed no significant difference between M0, M1 and M2 macrophages (Fig. 7A). In order to understand the kinetics of release, we analyzed monocytes treated with MSCF or tumor supernatants for 1, 3 and 6 days. Osteoactivin release was very low at day 3 and much higher at day 6 (Fig 7B), indicating that the shedding requires some time to occur.
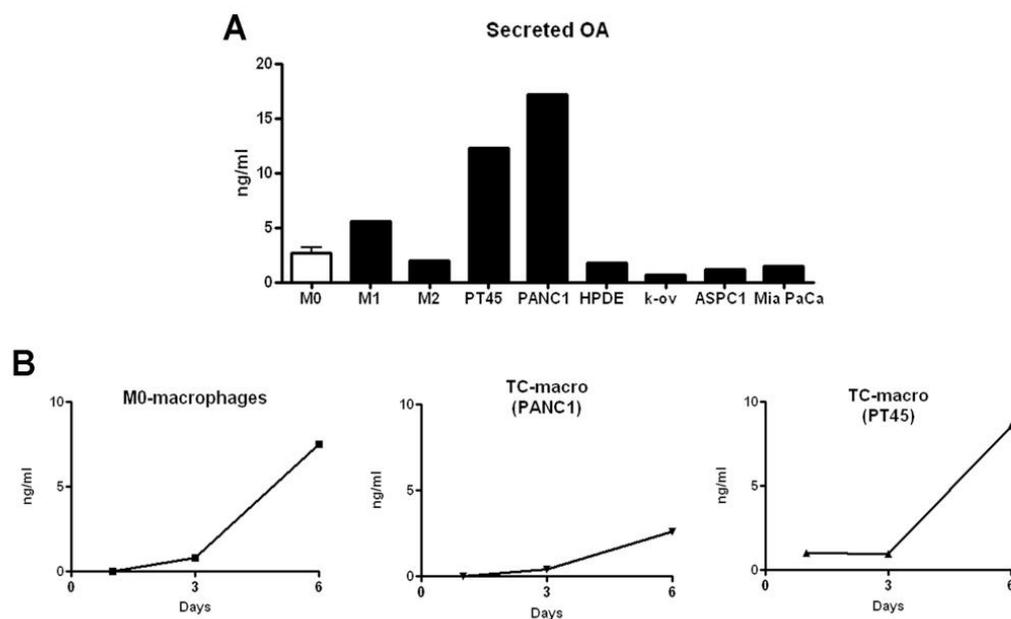
Fig 7. Elisa quantification of the soluble form of human Osteoactivin . A) Production of Osteoactivin in *in vitro* M-CSF-differentiated macrophages (M0), in M1/M2 polarized macrophages and in TC-Macrophages. B) Kinetics of OA production over 6 days. Representative results from different experiments are shown.

To confirm these data we repeated the above experiments with murine bone marrow-derived monocytes/macrophages. Unfortunately we have not found an antibody that worked so well for the

transmembrane isoform of murine OA; for this reason we could only evaluate the secreted form of the protein. We tested macrophage production of murine Osteoactivin (mOA) by MCSF-differentiated macrophages (M0), M1/M2 polarized macrophages, tumor-conditioned macrophages, as well as macrophages activated with LPS.

To obtain murine TC-macrophages we generated tumor supernatants from the pancreatic murine tumor cell line (PANC02), the mastocytoma cell line (P815) and three murine fibrosarcoma cell lines (MN-MCA1, MCA-1 and MCA-2). From our data we observed that Osteoactivin production was similarly induced in MCSF- macrophages, M1 and M2 macrophages, but was decreased in LPS stimulated ones (Fig 8A). Osteoactivin is also induced in TC-macrophages, with higher production with supernatants from PANC02 cells and the fibrosarcoma MCA-2 and MN/MCA1 (Fig. 8B).
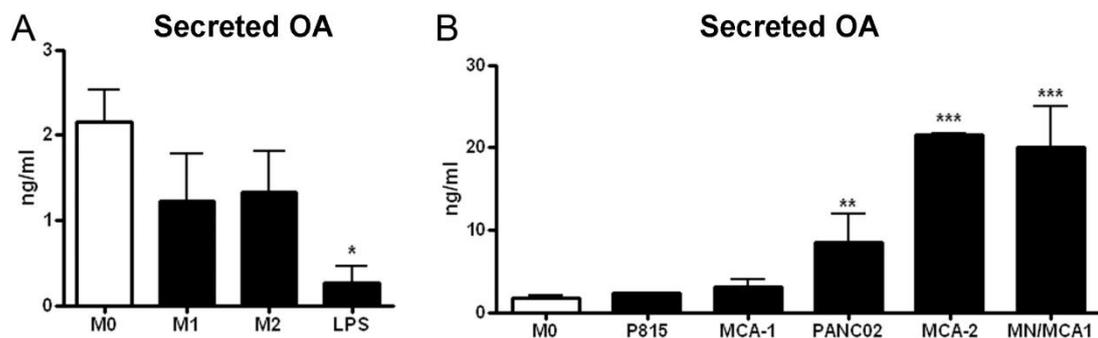
Fig 8. Elisa quantification of the soluble form of murine Osteoactivin . Production of osteoactivin by murine bone marrow derived macrophages; A) M-CSF-differentiated macrophages, M1/M2 polarized macrophages (treated as detailed in legend of Fig.7) and LPS stimulated macrophages . B) Production of Osteoactivin by murine tumor conditioned macrophages. Data are expressed as mean -/+ SD of 3 experiments. Statistical analysis: *p < 0.05, **p < 0.01, ***p < 0.001 (Student's t test).

Overall, these results demonstrate that Osteoactivin is expressed in human and murine macrophages and its expression is increased when they are exposed to tumor-derived factors, as it happens in the tumor environment. These findings suggested that Osteoactivin may have a functional role in the important cross-talk between macrophages and cancer cells, and prompted us to investigate this hypothesis in vivo in murine tumor models.

Biological role of Osteoactivin

Cell adhesion and migration:

Some reports, in the scientific literature, show that Osteoactivin is involved in important biological functions, such as cell adhesion, through its RGD domain and integrins, and also cell migration, in particular of with tumor cells [79, 80]. Therefore, we performed experiments to investigated if Osteoactivin could affect the adhesion and migratory properties of human monocytes and murine BM derived-monocytes.

In vitro adhesion assays were performed using recombinant Osteoactivin coated on plastic surfaces. Freshly isolated monocytes were plated onto the Osteoactivin layer and after 30 minutes of incubation the adherent cells were stained by Diff Quick kit and enumerated. We observed that Osteoactivin greatly enhanced the adhesive of human monocytes (Fig 9 A).

Moreover by a migration assay performed using transwell plates we observed that Osteoactivin could also function as a chemotactic factor inducing the migration of murine monocytes as efficiently as CCL2 that is considered a potent monocyte chemo-attractant (Fig 9 B).
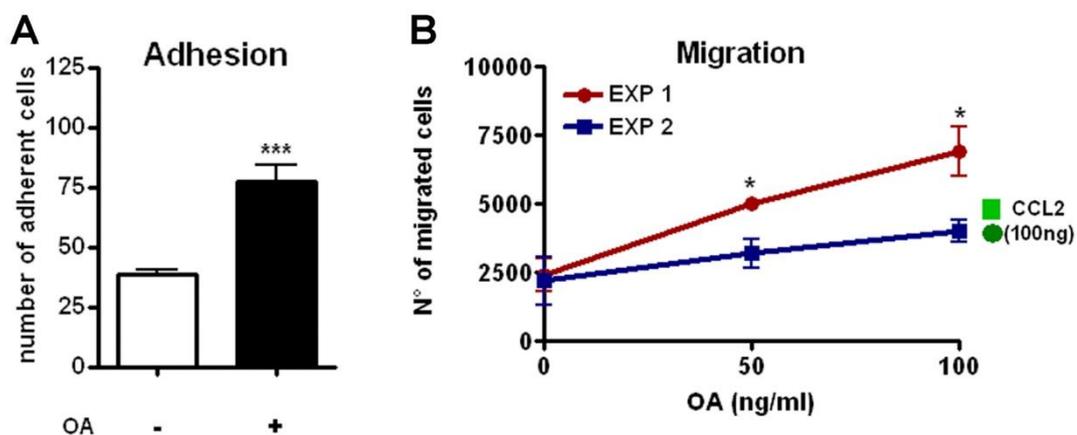
Fig 9. Monocyte adhesion and migration are enhanced by Osteoactivin . A) Adhesion assay on OA-coated wells. Human monocyte adhesion is enhanced by recombinant Osteoactivin (+); data are shown as number of plastic adherent cells (OA 2ug/ml); Mean ± SE for 3 replicates. B) Migration assay. Murine monocyte migration is induced by Osteoactivin (50 and 100 ng/ml), two experiments are shown (red and blue line). CCL2 (100 ng/ml) was used as reference chemo-attractant (green dot and square); data are shown as number of monocytes migrated through 5 μm pore size transwell filter. Statistical analysis: $p < 0.05$, ***$p < 0.001$ (Student's t test).

Macrophage differentiation and polarization:

In the scientific literature, Osteoactivin is described as a key regulator of bone biology, especially during the differentiation of osteoblasts and osteoclasts [69]. Using recombinant Osteoactivin as differentiation or polarization factor, we investigated the possibility that this protein could modulate monocyte-macrophage differentiation or M1/M2 macrophage polarization.

To test this hypothesis we evaluated the expression of the typical markers of differentiated macrophages (CD68/F4-80) and M1/M2 macrophages (MHCII and CD206) on our monocytes stimulated with soluble Osteoactivin during the culture period. Our results indicated that the recombinant protein had no significant effect on myeloid cell differentiation and neither on macrophage polarization (data not shown).

Taken together the results indicate that Osteoactivin is an interesting molecule expressed and released by tumor-conditioned macrophages both in humans and mice, involved in the stimulation of their migration and adhesion ability.

Mice of the DBA/2J strain lack functional Osteoactivin

To investigate *in vivo* the functional role of the protein Osteoactivin we took advantage of the mouse strain DBA/2J which displays a non-functional mutation in the *Gpnmb* gene. The point mutation (*Gpnmb*R150X) introduces a premature stop codon with the consequent formation of a truncated non-functional protein [70].
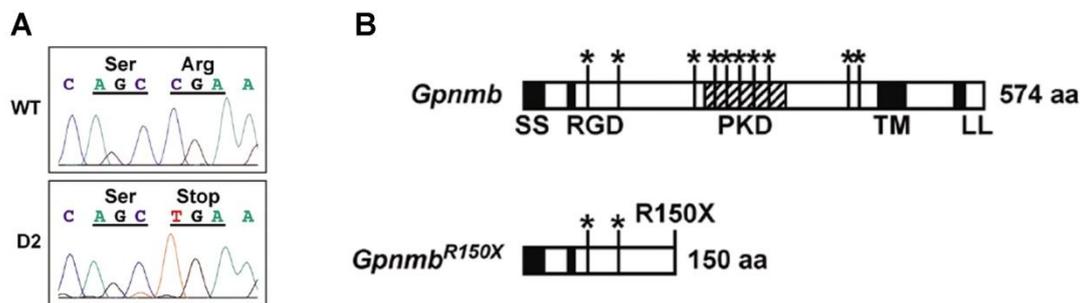
Fig 10. *Gpnmb* gene mutation in DBA/2J strain. A) Sequence comparison of *Gpnmb* products amplified from wild type (WT) and DBA/2J (D2) tissues indicating the presence of a premature stop codon mutation: *Gpnmb^{R150X}*; B) Representation of Osteoactivin precursor protein and the predicted truncated protein encoded by *Gpnmb^{R150X}* [70].

The phenotype of Osteoactivin -defective mice (DBA/2J) does not show obvious major problems, with the exception of the known rapid onset of glaucoma. In fact, aging mice develop iris pigment dispersion (IPD) by sloughed off pigment cells, retinal ganglion cell loss and optic nerve head excavation[70]. Furthermore, the Jackson Company generated a transgenic mouse line reconstituted with the native functional protein: DBA/2J-*Gpnmb$^+$* mice. Therefore, both mice with non-functional Osteoactivin and mice with the functional protein were available for this study.

Characterization of the monocyte/macrophage lineage in DBA/2J and DBA/2J Gpnmb[+]

Before using the DBA/2J and DBA/2J Gpnmb[+] mice in tumor models *in vivo*, we performed a general characterization of immune cells in these two strains, with a particular focus on the monocyte/macrophage lineage. Both the scientific literature and our results indicated that the two mouse strains had similar levels of circulating monocytes and spleen macrophages (not shown).

To analyze general functions of macrophages from these mice, we generated *in vitro* differentiated macrophages from bone marrow-derived monocytes stimulated with M-CSF, and investigated the production of the principal macrophage products induced by different stimuli, including LPS and PamCys. Tab.1 shows the quantification of the principal cytokines produced by treated monocytes in DBA/2J or DBA/2J Gpnmb[+] mice. With LPS stimulation, only monocytes from DBA/2J Gpnmb[+] are able to produce chemokines such as KC, CCL3, CCL5 and eotaxin, and cytokines: IL-1b, IL-6, IL-10 and IL-12. Cells from DBA/2J mice are completely unresponsive to LPS. On the contrary both DBA/2J than DBA/2J Gpnmb[+] monocytes are able to respond to PamCys with the production of all the cytokines tested. Thus, our results highlighted a defective response of the DBA/2J strain to LPS.

	LPS		PAM-CYS	
	DBA2J	DBA2J/GPNMB[+]	DBA2J	DBA2J/GPNMB[+]
IL1β	0,0	1,8	5,4	5,1
IL6	0,0	0,7	2,3	2,0
IL10	0,0	0,9	4,6	2,7
CCL3	0,7	4,5	22,6	18,0
CCL5	0,0	3,6	2,4	1,8
KC	0,0	4,3	25,6	29,0
Il12 P40	0,0	3,2	6,1	4,0
IL12 p70	0,0	0,8	2,3	2,1
Eotaxin	0,0	2,1	8,6	8,0

Tab 1. Cytokine production by *in vitro* monocytes from DBA/2J and DBA/2J Gpnmb[+] mice. When stimulated with LPS (24 hr), only monocytes from DBA/2J Gpnmb[+] mice are able to produce high levels of chemokines and cytokines. Upon stimulation with PamCys, monocytes from both DBA/2J and DBA/2J Gpnmb[+] mice respond equally well with higher production of the principal inflammatory mediators. Data are expressed in ng/ml.

As shown in Tab.2, also M1/M2 polarized macrophages from DBA/2J mice were unresponsive to LPS and did not produce any cytokine, with the exception of CCL2. Cytokine production was in general higher in M1/M2 macrophages derived from DBA/2J Gpnmb+ mice.

	M1		M2	
	DBA2J	DBA2J/GPNMB+	DBA2J	DBA2J/GPNMB+
IL1β	0,0	3,1	0,0	1,5
IL10	0,0	1,5	0,9	3,3
IL17	0,0	0,9	0,0	1,4
IL13	0,0	1,8	0,0	1,3
CCL3	0,0	5,7	0,0	1,3
CCL4	0,1	11,4	0,0	0,8
Eotaxin	0,4	4,8	6,2	6,2
CCL2	8,9	26,9	7,3	10,3
TNFα	0,0	0,6	0,0	0,7

Tab 2. Cytokine production by *in vitro* polarized macrophages from DBA/2J and DBA/2J Gpnmb+ mice. Only M1/M2 polarized macrophages taken from DBA/2J Gpnmb+ mice are responsive to LPS/IFNγ stimulation. Data are expressed in ng/ml.

It would be very interesting perform an accurate characterization of the monocyte/macrophage lineage in DBA/2J and DBA/2J Gpnmb+ to better understand differences in the inflammatory response of these cells, with particular attention to the LPS –TLR pathway. In the literature, in fact, there are contrasting results on the expression of TLR in these strains and their response to LPS [81, 82].

Osteoactivin in the tumoral context

To understand the role of Osteoactivin in the tumoral context we tested different *in vivo* tumor models taking advantage of the availability of the two different mouse strains.

We first tested the P815 cell line, a murine mastocytoma syngeneic for the DBA/2J strain. P815 cells (10^6 cells) were injected intraperitoneally (i.p.) in DBA2J and in DBA/2J Gpnmb$^+$ mice. We observed that in both groups animals developed a similar amount of ascites and similar tumor load (Fig 11A) These tumors did not present differences also in the tumor microenviroment composition as observed by FACS analysis (Fig 11B).
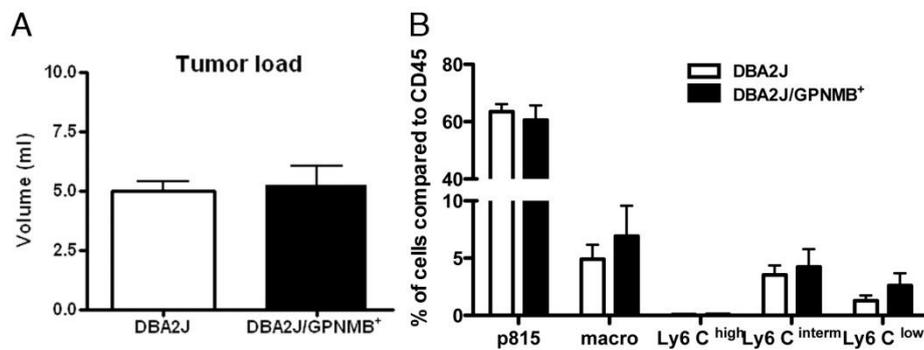
Fig 11. P815 trasplantable tumor model. A) Amount of intraperitoneal ascites at 14° day after tumor cell injection; the total volume is similar in DBA/2J and DBA/2J Gpnmb$^+$ mice. Data are shown as volume (ml) as means ± SE); B) Percentage of cell content into tumor ascites. The amount of tumor cells and macrophages is similar into both mouse strains. Data are shown as % of cells compared to total CD45 positive cells (Mean means ± SE).

The low availability of murine tumor models syngeneic for this particular strain prompted us to develop a carcinogenesis model upon treatment with the carcinogen methylcholanthrene (MCA). A subcutaneous injection of 500ug 3MCA was given to DBA/2J and DBA/2J Gpnmb$^+$ mice. Mice were constantly monitored for four months for the generation of MCA-induced fibrosarcoma. The two groups developed primary tumors starting from 16 weeks after MCA injection; no significant differences were observed in terms of tumor incidence and mean size of the tumors was comparable (data not shown).

Although we did not observe any particular difference in the two groups, this experiment has been useful to establish *in vitro* cells from the primary tumors: we expanded and established as proliferating cell lines two tumors originated from DBA/2J mice (G2 and G3 cell lines) and two from DBA/2J Gpnmb[+] mice (G4 and G5 cell lines).

To confirm that the cell lines were indeed stable and to assess their capability to re-grow *in vivo* we performed a transplantation experiment with two of the four selected fibrosarcoma cell lines: G2 cells (from DBA/2J) and G4 cells (from DBA/2J Gpnmb[+]). Tumor cells ($5x10^5$) were intramuscularly injected in each respective syngeneic mouse. All mice developed tumors within 15 days as shown in Fig 12 A-B.
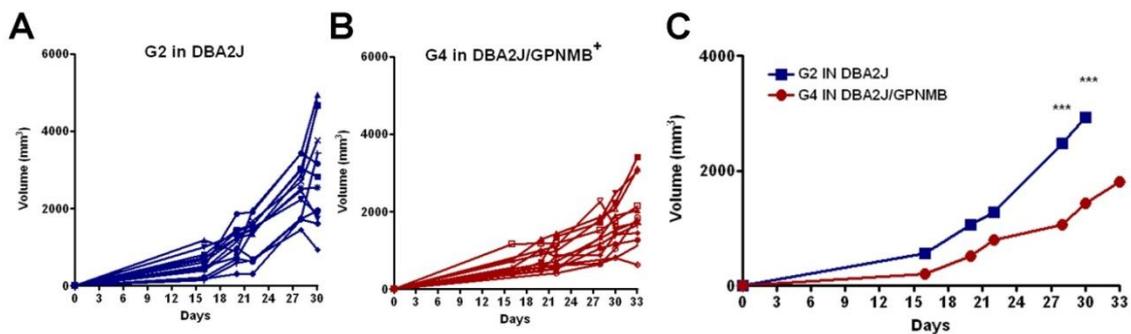
Fig 12. G2 and G4 Transplantable tumor model. A and B) Tumor growth curves of G2 cells (DBA/2J) and G4 cells (DBA/2J Gpnmb[+]) into their syngeneic mice, respectively; in the two graphs each line represent an individual tumor. C) Mean values of tumor volume of G2 and G4 tumors (10 mice per group). Data are expressed in mm^3 of volume determined by external caliper. Statistical analysis: ***p < 0.001 (Student's t test).

Although tumor growth in mice was highly heterogenous, likely because this was the first transplantation experiment with these primary fibrosarcoma, it was apparent that the two tumor cell lines had a different rate of proliferation. G2 tumors were growing more rapidly compared to G4 tumors and formed larger masses (Fig. 12 C). G2 tumors originate from DBA2/J mice with non-functional Osteoactivin , while G4 tumors were generated in DBA/2J Gpnmb[+] mice, which are able to produce a functional protein. Nevertheless, no hypothesis are worth mentioning at this stage on a

possible impact of Osteoactivin on the *in vivo* tumor growth, as this difference could be ascribed to intrinsic properties of the originally transformed cells.

In order to understand whether Osteoactivin is a pro-tumoral or antitumoral protein, we injected G2 tumor cells (Osteoactivin-defective) in DBA/2J Gpnmb[+] mice (Osteoactivin competent) and in in DBA2J mice for comparison. To better appreciate possible differences in tumor incidence and growth rate, we reduced the number of injected tumor cells ($5x10^4$). We injected cells intramuscularly and monitored mice over time for tumor development. Six weeks later, the incidence of tumor take was 38.5% in DBA/2J and 50% in DBA/2J Gpnmb[+] mice. Some of the tumors in DBA/2J Gpnmb[+] mice proliferated remarkably faster forming very large masses and disseminated to the lungs.

Fig 13. G2 trasplantable tumor model in DBA/2J and DBA/2J Gpnmb[+] mice. A and B) Tumor growth curve after injection of $5x10^4$ G2 (OA neg) cells into DBA/2J and DBA/2J Gpnmb[+] mice. Data are expressed in mm^3 of volume determined by external caliper. Upon an initial similar growth rate, after 6 weeks tumors grew more rapidly in DBA/2J Gpnmb[+] . C) Tumor incidence expressed as percentage of mice developing tumors. E) Number of lung metastasis. Each dot represents an individual mouse.

31

These results clearly indicated that Osteoactivin expression in the stromal microenvironment, perhaps by macrophages, may provide a proliferative advantage to tumor cells which acquire a more aggressive phenotype *in vivo*.

Considering the observed effect of Osteoactivin in the tumor microenvironment and given that its expression is increased in several types of cancer, we decided to directly engineer MCA-OA⁻ cells to express the native protein and obtain isogenic cell lines expressing or not Osteoactivin.

We cloned the murine *gpnmb* gene and expressed it in a lentiviral pRRL Sin plasmid in which egfp has been replaced with mCherry (Fig 14A); we transduced two different MCA-OA⁻ cell lines (G2 and G3). mCherry-positive cells were selected by FACS sorting, propagated and checked for OA expression on cell membrane and for the secreted form. Both G2 and G3 cell lines were successfully transduced. As G2 cells showed better results, we decided to use this cell line in future experiments. Fig 14 shows that the G2 trasduced with Osteoactivin cells, called G2 OA, highly expressed both the transmembrane form (Fig 14B) and the secreted protein (Fig 14C). Fig 14D shows by confocal microscopy the expression of the cherry-linked transgene: the protein Osteoactivin is mainly localized on the cell membrane, while in MOCK-transduced cells (G2 MOCK) the mCherry dye is mainly intra-cytoplasmic.
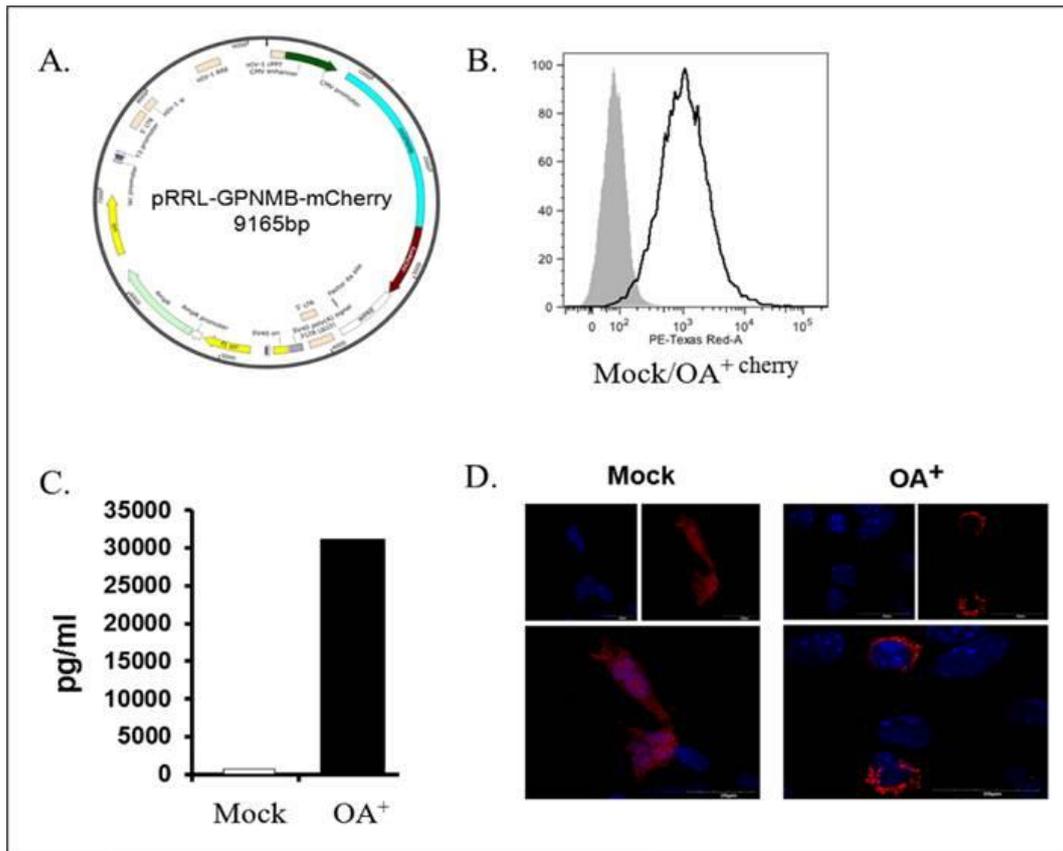
Fig 14. Characterization of OA-transduced G2 cell line. A) Scheme map of the lentiviral plasmid; B) FACS profile plot of transmembrane Osteoactivin in G2 OA (black line) and G2 MOCK-transduced cells (grey profile); C) Quantification of soluble isoform of Osteoactivin in G2 OA and G2 MOCK-transduced cells; D) Confocal images of Osteoactivin in G2 OA and G2 MOCK transduced cells (OA in red - DAPI in blu).

G2 OA and G2 MOCK cell lines were initially characterized *in vitro*. Both cell types had a stable and similar rate of proliferation as evidenced in growth curve experiment within the short period of 72 hrs (not shown). The next step was to evaluate if the presence/absence of Osteoactivin within tumor cells could affect tumor growth *in vivo* in mice. To this purpose we inoculated G2 OA and G2 MOCK cells *in vivo*.

We first used NOD/scid IL2Rg^{null} (NSG) immunodeficient mice, to avoid the possibility that the OA protein could be recognized as "foreign" by DBA/2J immunocompetent mice. Tumor cells (10^5) were intra-muscularly injected and tumor growth followed over time. Surprisingly, tumors from G2 OA cells were already palpable after 10 days, while tumors from G2 MOCK cells appeared around day 15-20 (Fig 15A). Osteoactivin-transduced tumors grew more rapidly than

MOCK cells and tumor weight was significantly higher at sacrifice (Fig 15B). Furthermore G2 OA tumors disseminated to the lungs and formed more metastasis compared with MOCK tumors (Fig 15C). These results in NSG mice indicated that tumor cells producing Osteoactivin had features of more aggressive tumors as far as proliferation rate *in vivo* and spreading to distant organs.
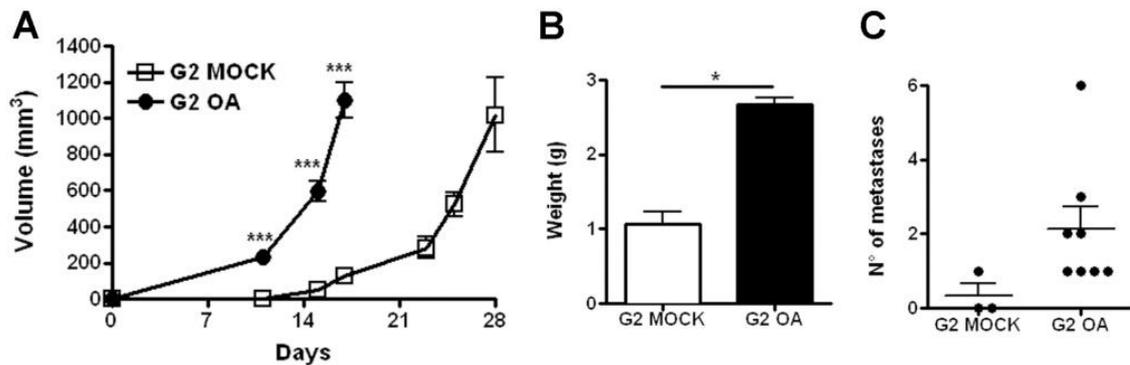

Fig15. G2 OA/ G2 MOCK transplantable tumor model in NSG mice. A) Tumor growth curve after inoculation of 10^5 G2 OA or G2 MOCK cells into NSG mice. Data are expressed in mm^3 of volume determined *in vivo* by external calliper. B) Tumor weight of tumors. C) Number of formed lung metastasis. Each dot represents an individual mouse. Results are from one representative experiment of three performed with similar results. Statistical analysis: *p < 0.05, ***p < 0.001 (Student's t test).

We next investigated by immunoistochemistry (IHC) the presence of macrophages and blood vessels, in order to study the composition of the tumor microenviroment. Surprisingly G2 OA tumors had significantly lower levels of F4/80$^+$ macrophages and CD31$^+$ vessels compared to MOCK tumors (Fig 16). The finding that more aggressive tumors (G2 OA) contained fewer macrophages, compared to their counterpart, was unexpected, especially because our previous experience with MCA-induced tumors evidenced that the microenviroment is highly populated by TAM, and their presence is usually associated with pro-tumoral functions [83]. To go more in depth in the characterization of the microenviroment composition of OA-transduced tumors, we evaluated also the presence of activated fibrobasts and collagen deposition by IHC. We observed that G2 OA tumors were richer in collagen content and density of SMA$^+$ activated fibroblasts compared to MOCK tumors as shown in Fig 16.
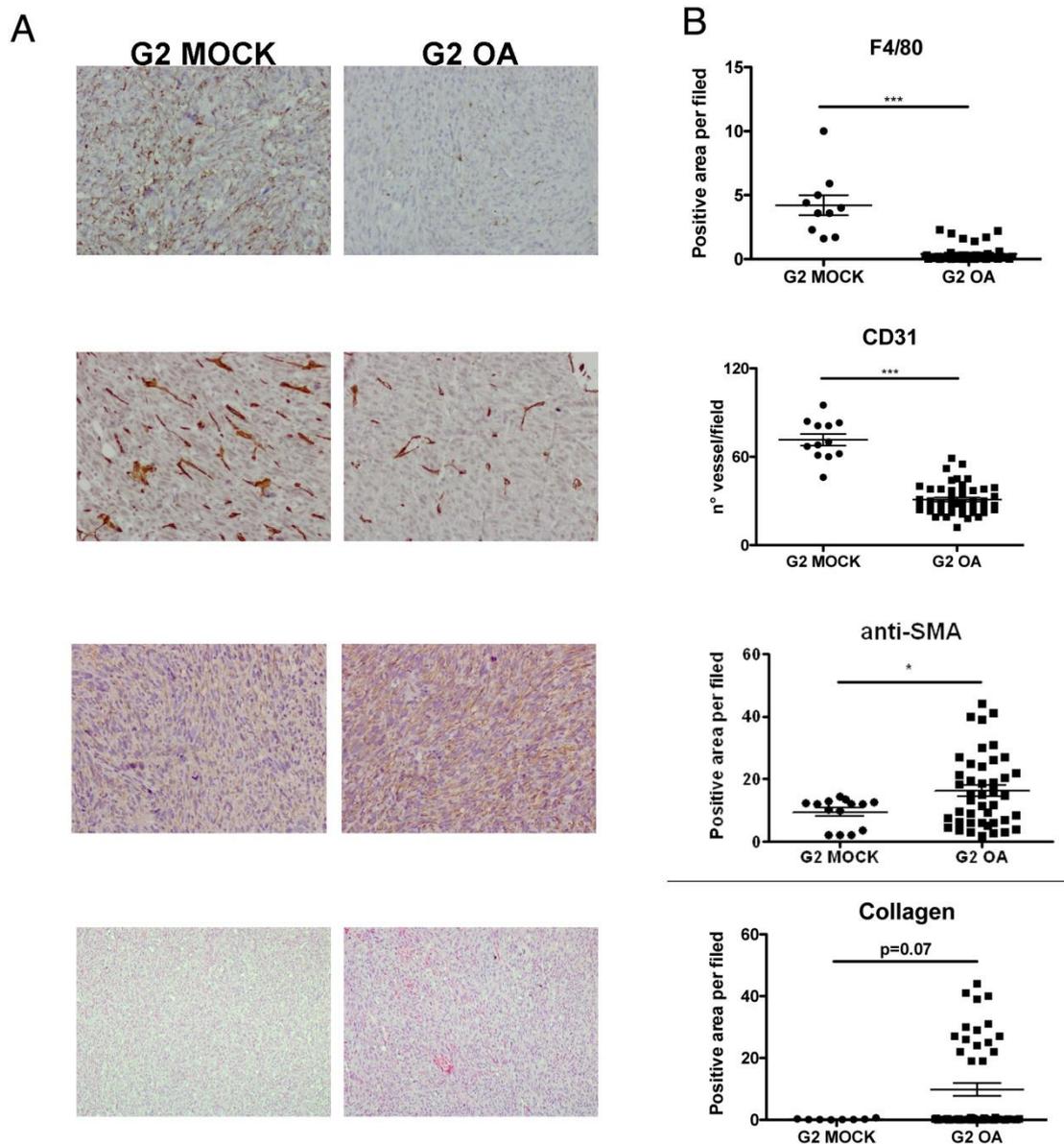
Fig 16. Immunoistochemistry analysis of G2 OA and G2 MOCK tumors from NSG mice. A) Representative IHC images of tumor sections stained for F4/80, CD31, SMA and Collagen (Sirius red) at original magnification 20X. B) Immunoistochemistry analysis**.** Results are calculated as mean of five microscope fields for each sample. Images were analyzed using Image-ProAnalyzer software. The positive area for macrophages (F4/80^{+}) and the number of vessels (CD31^{+}) are higher in G2 MOCK tumors comapred to G2 OA. On the contrary, the numbers of activated fibroblasts (SMA^{+}) and collagen content (Sirius red[+]) are higher in G2 OA tumors. Statistical analysis: *p < 0.05, ***p < 0.001 (Student's t test).

To reinforce the above results of lower amount of TAM and vessels and higher density of activated fibroblasts, we performed *real-time* PCR on samples collected from G2 OA and G2 MOCK tumors from NSG mice to quantify mRNA levels of the principal macrophages markers,

such as CD68 or CD163, chemotactic factors CCL2 or VEGF, fibroblastic factors, such as EGF and FGF, and MMP2 a protease involved in ECM degradation. As shown in Fig17 it was confirmed that CD68 and CD163 levels were lower in G2 OA tumors compared to MOCK ones (Fig 17A). RNA levels of CCL2, a major chemotactic factor for macrophages, were also decreased, at least partially explaining the lower density of TAM in these tumors (Fig17A). On the other hand, RNA levels of MMP2, EGF and FGF were increased in G2 OA tumor samples, and the results are in line with the higher amount of activated fibroblasts observed by immunohistochemistry (Fig 17B).
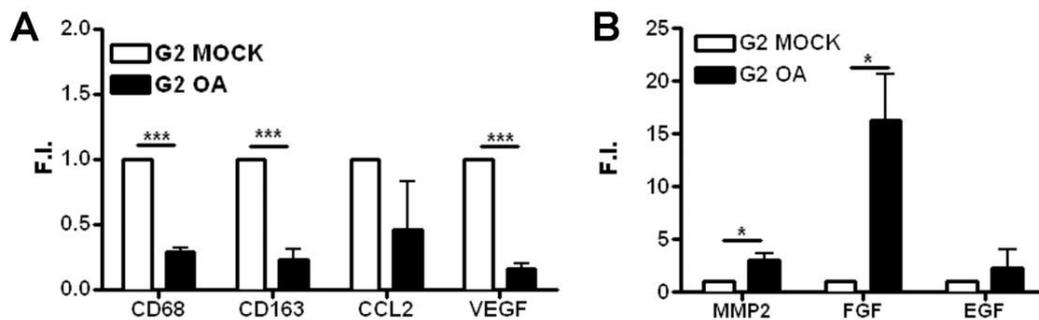
Fig 17. mRNA levels in G2 OA and G2 MOCK tumor samples. (A) Expression levels of macrophage markers CD68 and Cd163, CCL2 and VEGF in tumors of NSG mice. (B) Expression levels of metalloprotease-2 and fibroblasts-related growth factors. Statistical analysis: $*p < 0.05$, $***p < 0.001$ (Student's t test).

To evaluate whether the tumor cell line expressing Osteoactivin could be able to grow faster also in immunocompetent mice, we next performed the same type of experiment using the syngeneic DBA2/J mice. G2 OA and G2 MOCK cells were intramuscularly inoculated (10^5). Tumors grew slowly and for the first three weeks both types of tumors had the same proliferation rate (Fig 18A). However, after 3 weeks the volume of G2 OA tumors was larger, as well as tumor weight at sacrifice (Fig 18B); G2 OA tumors disseminated to lungs in some mice, while G2 MOCK tumors never formed metastasis (Fig 18C).

**Fig 18. G2 OA/G2 MOCK transplantable tumor model in DBA/2J mice. A**) Tumor growth curve after inoculation of 10^5 G2 OA or G2 MOCK cells into DBA/2J mice. Data are expressed in mm³ of volume determined *in vivo* by external caliper; B) Tumor weight at sacrifice. C) Number of lung metastasis, each dot represents an individual mouse. G2 OA tumors have higher proliferation rate and formed more metastases than G2 MOCK tumors. Graphs are a representation of two independent experiments, with similar results. Statistical analysis: *p < 0.05, **p < 0.01, (Student's t test).

The immunohistochemistry of tumor sections again revealed that OA-expressing tumors contained lower amounts of macrophages and vessels, and higher density of activated fibroblasts (Fig 19). Collagen staining did not reveal any differences in the two groups (data not shown), this is probably due to the fewer amount of activated fibroblasts in these tumors compared to tumors derived from NSG mice. Similarly to what we observed in NSG mice by *real-time* PCR, we found that G2 OA tumors had lower amount of CD163 and CCL2, but not of CD68 or VEGF. Moreover MMP2 is much more expressed in G2 OA tumors, compared to G2 MOCK cells, while there is only a slight increase of EGF and FGF (Fig. 20). Overall, these results in syngeneic immunocompetent mice are in line with the immunohistochemistry analysis previously performed in immune-deficient NSG mice (shown in Fig 16).

Fig 19. Immunoistochemistry analysis of tumors taken from DBA/2J mice. A) Representative IHC images of tumor sections stained for F4/80, CD31, and αSMA at original magnification 20X. B) Immunoistochemistry analysis. Results are calculated as mean of five microscope fields for each sample. Images were analyzed using Image-ProAnalyzer software. The positive area for macrophages (F4/80^{+}) and the number of vessels (CD31^{+}) are higher in G2 MOCK tumors compared to G2 OA. On the contrary the number of activated fibroblasts (SMA^{+}) is higher in G2 OA tumors. Statistical analysis: *p < 0.05, ***p < 0.001 (Student's t test).
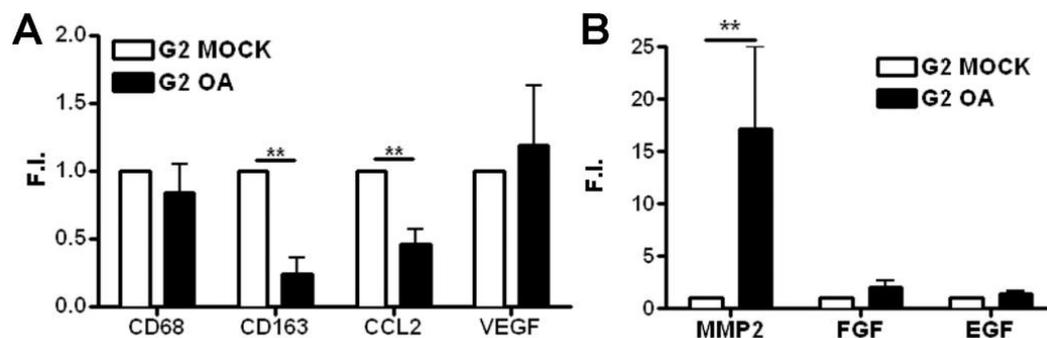

Fig 20. mRNA levels in DBA/2J tumor samples. (A) Expression levels of macrophage markers CD68 and Cd163, CCL2 and VEGF and (B) of MMP2, FGF, EGF in tumors from DBA/2J mice. Statistical analysis: **p < 0.01, (Student's t test).

So far the results demonstrated that tumor cells producing Osteoactivin grew differently in vivo compared to non-expressing cells, in both immune-deficient and immune-competent mice, showing a higher proliferation rate and metastatic behaviour.

We therefore started to suspect that Osteoactivin-producing tumors contain a higher proportion of tumor-initiating cells. To test this hypothesis, we performed an *in vivo* experiment inoculating a very low number of tumor cells. As low as 10^3 G2 OA and G2 MOCK cells were injected in NOD/scid IL2Rg^{null} (NSG) mice testing their tumorigenicity. Surprisingly, as shown in Fig.21, G2 OA tumors were already detectable starting from the 15th day post-injection, much earlier than the MOCK counterpart.
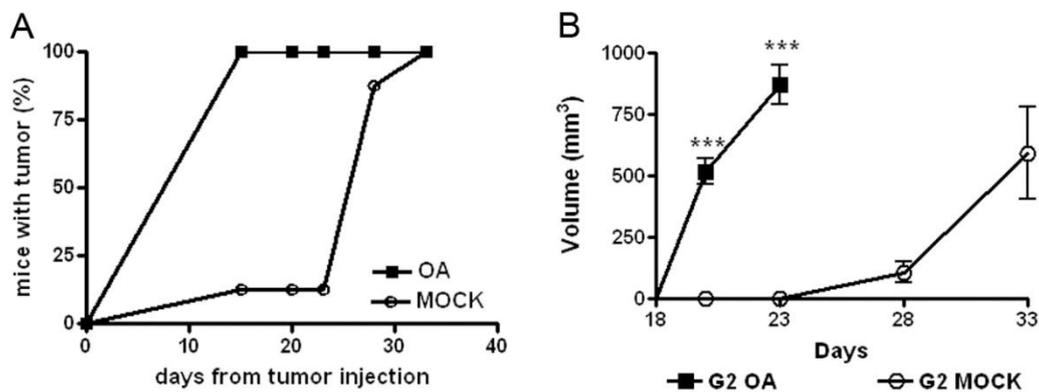

Fig 21. Tumorigenicity of G2 OA and G2 MOCK tumors in NSG mice. *A)* Tumor growth curve after inoculation of 10^3 G2 OA or G2 MOCK cells in NSG mice. G2 OA tumors grow much more rapidly than G2 MOCK ones. B) Tumor volume expressed in mm^3 of volume determined *in vivo* by external caliper. Statistical analysis: ***p < 0.001 (Student's t test).

The results indicate that Osteoactivin provide tumor cells with a proliferative advantage so that even a small number of cells could rapidly develop and form tumors in vivo. Overall these findings are in line with those observed in the previous experiments, where OA-negative tumor cells grew faster and more aggressively in DBA/2J Gpnmb$^+$ mice; in these mice, Osteoactivin can be produced by the stromal compartment, including macrophages. Therefore we conclude that either when endogenously produced, or when secreted in the tumor milieu, this protein has pro-tumor functions and facilitates tumor development.

In vitro characterization of engineered cell lines

Starting from the observation of the different pattern of *in vivo* growth and higher tumorigenicity of G2 OA cells, we further characterized *in vitro* the proliferation rate of our engineered cell lines, in a longer assay than previously performed, and their ability to survive under non-optimal conditions. After plating, cells were counted every 24h without change of medium. Until 72 hours we did not observe any differences in term of growth; in contrast, after 4 days MOCK cells started to die, while Osteoactivin-expressing cells continued to grow actively (Fig 22 A). These data indicate that under conditions of nutrient/serum deprivation, G2 MOCK cells progressively die, while G2 OA cells are able to survive. Furthermore, after a period of 96 hours, G2 OA cells gradually detached from plastic surface and were able to proliferate in an anchorage-independent manner, giving rise to spheroids (Fig 22 B).
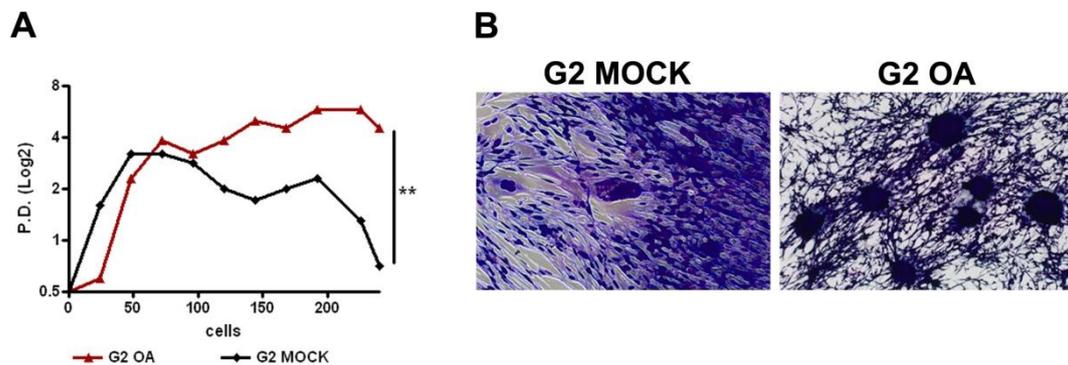

Fig 22. *In vitro* growth of G2 OA and G2 MOCK cells. A) growth curve of G2 OA and G2 MOCK cells; G2 OA cells (red line) grow with a more rapid rate compared to G2 MOCK counterpart (black line); Data are expressed as population doubling (PD) that represents the number of cell duplications. The growth curve started from $2x10^5$ cells. Statistical analysis: **$p < 0.01$, (Student's t test). **B)** Representative picture of spheroids formed by G2 OA cells after one week of culture. On the left side the monolayer formed by G2 MOCK cells.

Considering that the ability to form sphere is a typical feature of stem cells, we decided to switch the usual culture medium (RPMI1640) with the Iscove medium without FBS and supplemented with specific factors: mEGF, mFGF, B27 and N2. Under these conditions, we observed that all G2 OA cells were able to form spheres, while only 30% of G2 MOCK cells did

so. In order to check their self-renewing ability, spheres of G2 OA and G2 MOCK cells were harvested, trypsinized to have single cell suspension and re-plated in culture; a second round of subsphere-forming assay was performed. Only G2 OA cells were able to form secondary and tertiary spheres while MOCK cells did not have this self-renew ability (Fig 23).
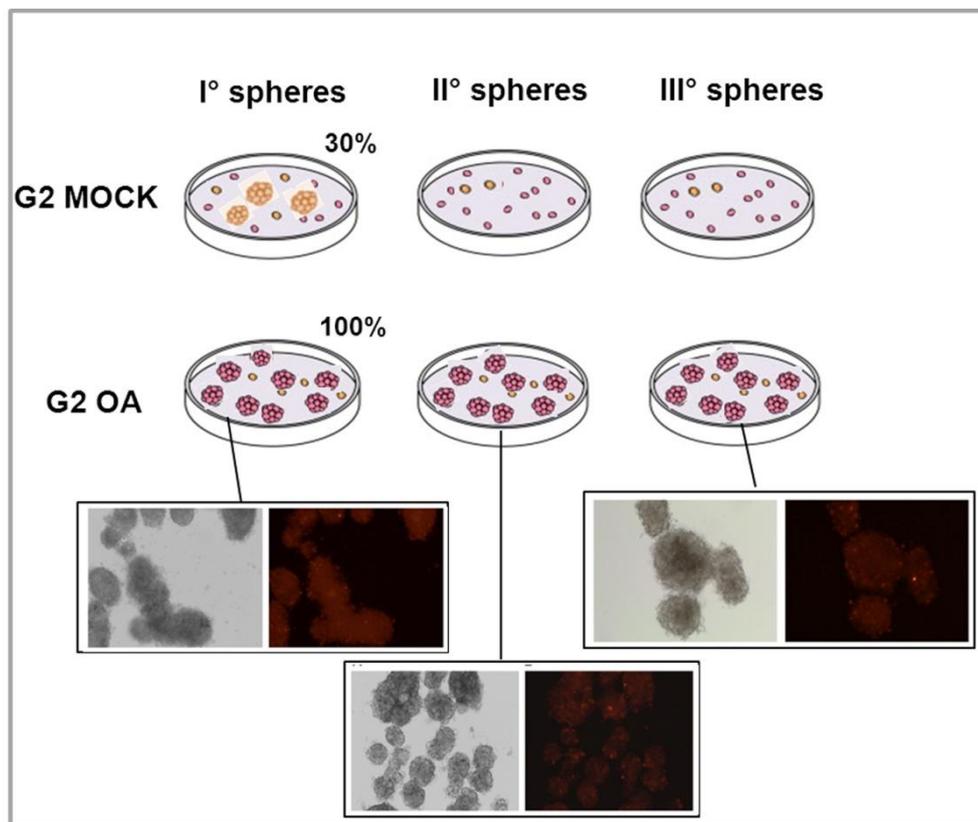

Fig 23. Sphere-forming assay. G2 OA cells were able to form spheres, while only 30% of G2 MOCK cells did so (upper part of the picture). G2 OA cells are able to form secondary and tertiary spheres starting from a single cell suspension of their primary/secondary spheres. In the lower part of the figure representative pictures taken after a week of culture with light and fluorescence microscopy at magnification 20X that show primary, secondary and tertiary spheres formed by G2OA cells.

This self-renewal property prompted us to investigate in depth the expression of markers typical of tumor stem cells. Cancer stem cells do not have a unique set of markers because their expression depend on the nature of formed tumors. The pathological analysis on our tumor samples revealed that G2 MOCK and G2 OA cells form mesenchymal tumors. To test whether the sphere forming cells could be really cancer stem cells as we assumed, we studied the expression of typical

mesenchymal stem cell markers, such as CD44, Sca1, CD117 (c-Kit), CD135; we also tested typical hematopoietic stem cell markers (CD45, CD11b, F4/80 and CD34) and a generic stem cell marker: Sox2. We evaluated the expression of these markers in G2 MOCK, G2 OA adherent cells and G2 OA spheres. All the cells analyzed did not express hematopoietic markers, with the only exception of CD34; this protein was expressed in all the adherent cells, but decreased when they become spheres. Both G2 MOCK and G2 OA cells expressed CD44, but not CD135, both in adherent cells and in cells in suspension. Sca1 was expressed only in G2 OA cells (adherent or spheres), while in MOCK cells was present at very low levels. Two typical markers expressed by our spheres were CD117 and Sox2, their levels increased in secondary formed spheres (Fig. 24).

		Mock	OA	G2 OA primary spheres	G2 OA secondary spheres
Hematopoietic markers	F4/80	-	-	-	-
	CD45	-	-	-	-
	CD11b	-	-	-	-
	CD34	99,6	91,4	49,6	67,4
Mesenchymal stem cell markers	CD117	6,2	5,8	32,3	30,0
	Sca1	12,0	77,5	87,5	67,0
	CD44	71,1	95,6	60,7	50,0
	CD135	-	-	-	-
Stem cells marker	Sox2	0,8	0,8	15,7	50,0

Tab 3. Expression of cancer stem cell markers. Cytofluorimetric staining panel of G2 OA and G2 MOCK cells grown in Iscove medium (without FBS) supplemented with mEGF, mFGF, B27 and N2; Primary and secondary G2 OA spheres express high level of CD117, Sca1 and Sox2 and they are negative for the most part of the other markers we tested.
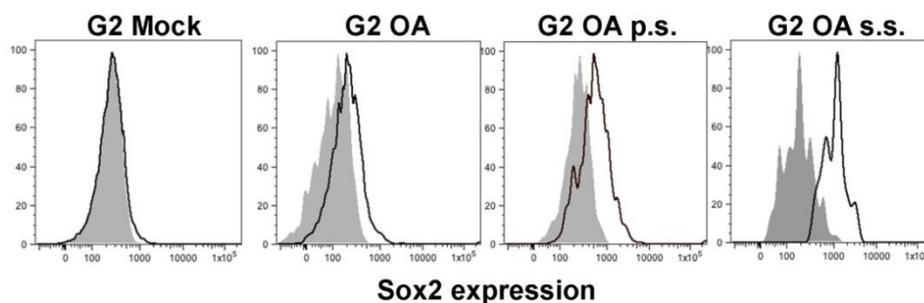

Fig 24. Representative profile of Sox2 expression. Primary and secondary G2 OA spheres express high levels Sox2.

We also evaluated the mRNA levels of the principal transcriptional factors typical of cancer stem cells; not surprisingly, we found that NANOG, OCT 3/4, DNMT and Brachyury were higher in G2 OA cells compared to G2 MOCK cells. In particular, their expression increased when G2 OA cells grew as spheroids, in fact mRNA levels resulted significantly higher in primary spheres as well as in secondary ones (Fig 28/25).
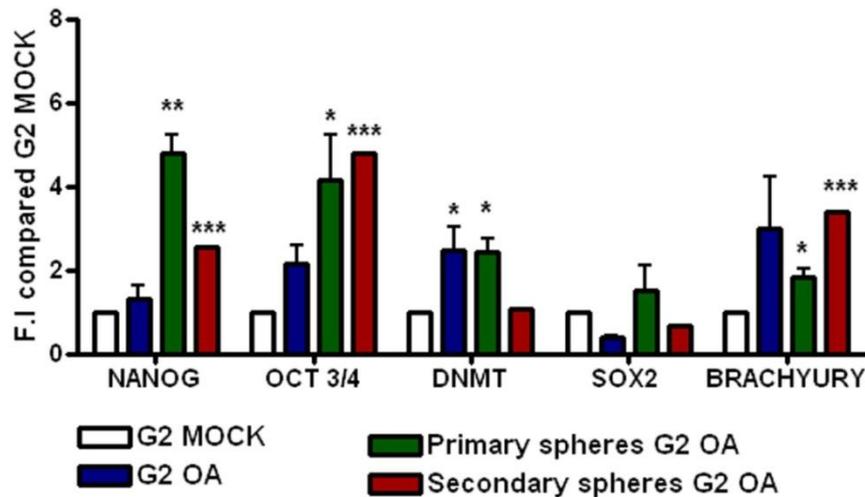

Fig 25. mRNA levels of stemness-related transcriptional factors. G2 OA cells (blue bars) express higher levels of OCT3/4, DNMT and Brachyury compared to G2 MOCK cells (white bars). The expression of these genes and the expression of NANOG increase when G2 OA cells grew as spheroids (green bars) and, in many cases, also in secondary spheres. Statistical analysis: *p < 0.05, **p < 0.01, ***p < 0.001 (Student's t test). All samples are tested in triplicate; Mean values ± SEM.

Taking advantage of the availability of in vivo-grown tumor samples from the above experiments, we performed other *real-time* PCR analyses to detect the typical transcription factors of stemness. We observed that NANOG, OCT 3/4, SOX2 and Brachyury were indeed overexpressed in G2 OA tumors compared to G2 MOCK tumors, with particular significant differences in samples grown in NSG mice (Fig 29).
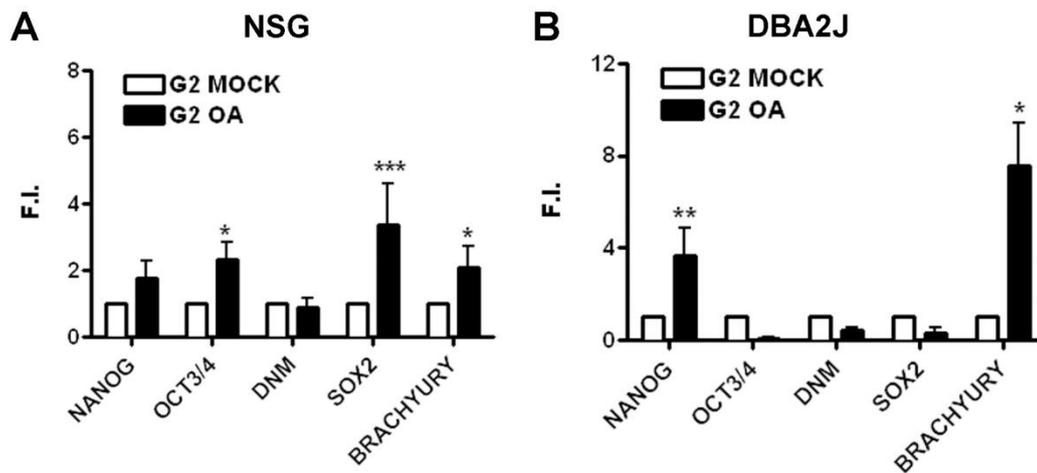
Fig 29. mRNA levels of stemness-related transcriptional factors. Principal transcriptional factors involved in cell stemness in G2 OA and G2 MOCK tumor samples in both NSG (A) and DBA/2J (B) mice (5 mice/group). The higher expression of NANOG, OCT 3/4, SOX2 and Brachyury by G2 OA tumors compared to G2 MOCK tumors is significantly different. Statistical analysis: *p < 0.05, **p < 0.01, ***p < 0.001 (Student's t test). In tumors of NGS mice, only NANOG and Brachyury are increased. Data are expressed as fold increase compared to G2 MOCK cells. All samples are tested in triplicates. Mean values ± SEM.

Collectively, our data demonstrate that the exogenous expression of Osteoactivin by tumor cells is associated with features of stemness. The up-regulation of typical stem cell markers, in Osteoactivin-producing cells, is likely related to their enhanced survival and proliferation ability, and higher tumorigenicity *in vivo*. These data bring us to speculate that also the Osteoactivin produced by tumor-associated macrophages might support cancer stem cells and enhance survival and proliferation of tumor cells.

DISCUSSION

Tumor-associated macrophages (TAM) represent a major leukocyte component of solid tumors and it is now established that they are key players in the buildup of the inflammatory microenvironment. TAM perform mostly pro-tumoral function supporting angiogenesis, tumor growth and metastatization processes and suppression of adaptive immune response. Pre-clinical and clinical evidence firmly demonstrated a correlation between high TAM density within tumor mass and poor patient prognosis for the majority of tumors [22-25].

In our study, from the analysis of a gene expression profiling of macrophages co-cultured with tumor cells (tumor-conditioned macrophages), we found that these cells are able to express and release a factor: *GPNMB*/Osteoactivin, which may be involved in the cross-talk between cancer cells and macrophages [59] .

In the scientific literature, Osteoactivin is presented as a protein expressed by several cell types and possibly involved in many physiological and pathological conditions. However, results on the functional activities of Osteoactivin are frequently conflicting. In normal tissues Osteoactivin has been described as "controller" of cell differentiation and cell adhesion especially in fibroblasts, epithelia and bone cells [69]. Some studies have described an immuno-regulatory function of this protein, either as inhibition of T cell activation [15], or in contrast, as stimulator of dendritic cell mobilization and defensive function against pathogens [84]. In the mononuclear phagocyte system Osteoactivin has been found expressed in the microglia of brain, where it exerts protective functions for neurons and in osteoclasts, where it participates in the maintenance of bone homeostasis.

In pathological conditions of tissue damage (kidney, liver, muscle) this protein is always upregulated and its presence is regarded as important for the healing tissue, probably via the scavenging of debris and activation of MMPs in the remodeling phase [75, 77]. Its absence in

experimental models is always associated with delay of tissue repair. In tumors, OA expression has been described in melanomas, gliomas and breast cancer.

Despite its original name (glycoprotein non-metastatic B) due to its first definition in low metastatic melanomas, it is now clear that Osteoactivin is expressed by highly malignant melanomas as well as in other tumors, and its expression has been linked with increased tumor growth, invasiveness and metastasis, especially in breast cancer, but opposite results have been described in prostate carcinomas [73, 85-87]. In recent years, attempts to target Osteoactivin therapeutically have been pursued: a clinically available anti-Osteoactivin antibody conjugated with the cytotoxin auristatin E has been developed and is currently under investigation in oncology trials in patients with melanoma and breast cancer [88].

Knowledge on the mechanism of action of this molecule is also insufficient. The transmembrane isoform contains a hemi-ITAM motif with a theoretical signaling capacity, though not formally demonstrated. The secreted form has been reported to bind to the receptor CD44 via ERK/AKT signaling [89]. The most consistent results in the literature define that this molecule favors cell-cell adhesion and cell mobilization, via RGD-integrin binding; these are important processes involved in several physiological and pathological conditions. An important determinant of the functional activity of this protein appears to be its state of glycosylation in the extra-cellular PKD domain, which adds a further level of complexity in the interpretation of the results obtained with the native and the recombinant produced protein.

In our study we found that Osteoactivin is induced upon M-CSF- driven macrophage differention and it is upregulated by anti-inflammatory stimuli. Instead, a study by Ripoll et al (2007) reported that Osteoactivin is induced in macrophages by LPS and IFNγ, a finding that we did not confirm, as our results clearly showed a down-regulation of this molecule by inflammatory stimuli. As a matter of fact, its expression in TAM, its upregulation by tumor supernatants and by IL-10, and its expression in resolving macrophages, more likely calls for a regulatory and tissue protective role for this protein [75].

Aim of our study was to identify the biological significance of Osteoactivin expression in macrophages conditioned by the tumor microenvironment.

The availability of commercial mouse strains with functional or non-functional protein: DBA/2J (OA-) and DBA/2J Gpnmb$^+$ (OA$^+$) mice was a real advantage for our experimental *in vivo* studies. As described above, the phenotype of Osteoactivin-defective mice (DBA/2J) does not show evident major problems, with the exception of the known rapid onset of glaucoma, but less is known about their immunological status. In this study we observed that monocytes and macrophages from DBA/2J mice are less responsive to LPS stimulation. In the literature, there are contrasting results on the expression and signaling functionality of the TLR4 receptor in DBA/2J mice. One study investigated the transcriptional program of macrophages from different mouse strains in response to LPS; the authors reported that, in spite of great variation in the number of modulated genes, DBA/2J mice had a similar profile compared to C57Bl6 mice [90]. Another study showed that BXD29 mice, which have a DBA/2J background, have a mutated TLR4 and attenuated response to LPS [81]. Thus, in addition to the well characterized C3H/HeJ strain with mutated TLR4, also DBA/2J mice may not optimally respond to bacteria. As far as susceptibility to pathogens, DBA/2J mice appear to be more susceptible than C57BL/6J mice to Streptococcus Group A infection, a Gram positive bacterium and also to viral infections such as several influenza virus subtypes. [91] [92]

The main reason to use DBA/2J mice in our study was the reported absence of a functional Osteoactivin protein in this strain. Using both the defective strain and the reconstituted DBA/2J Gpnmb$^+$ mice, we explored whether tumors were developing with a different growth rate. We first investigated a syngeneic transplantable tumor model: the P815 murine mastocytoma cell line, and found no significant differences in terms of tumor take and volume in the two mouse strains. In those experiments we injected a high number of cells (10*6) and this may have masked a small but important difference in tumor growth. In fact, with the fibrosarcoma model, we appreciated an accelerated tumor growth in DBA/2J Gpnmb$^+$ mice only when using a small number of injected tumor cells. We plan in the future to perform another experiment with a lower number of P815

cells to verify if also in this model we can appreciate more tumor rapid growth in Osteoactivin-competent mice.

As DBA/2J syngeneic tumor models are very few, we decided to generate primary tumors in the two mouse strains by chemical carcinogenesis. This was also informative regarding the incidence of neoplastic transformation, which was, however, similar in OA-proficient and deficient mice. Some of the chemically-induced fibrosarcoma that developed after some months were re-transplanted to generate tumor cell lines stably growing in vivo. In particular, an informative experiment was to inject a fibrosarcoma generated in DBA2/J OA-deficient mice, in OA-proficient animals. We observed higher tumor take and faster tumor proliferation compared to tumors grown in DBA/2J mice. These results suggested that Osteoactivin expression in the tumor micro-environment by macrophages or stromal cells of DBA/2J Gpnmb$^+$ mice might be able to support tumor growth.

To directly investigate the biological effect of Osteactivin on tumor development, we engineered OA$^-$ tumor cells to express the native protein, with the aim to verify if OA-expressing cancer cells had a different growth pattern *in vivo*. This was indeed the case, with remarkably earlier and faster tumor growth *in vivo* and higher metastatic capacity compared to MOCK-transduced cells. These results were consistent both in the syngeneic strain and in immunodeficient NSG mice. The finding that Osteoactivin expression correlated with more aggressive tumor behavior is in line with literature data as reported by Rose et al [73, 93].

An unexpected finding in our studies was the fact that tumors formed by OA-transduced cancer cells contained significantly lower numbers of macrophages. Our group has quite a good experience in the characterization of macrophages infiltrating chemically-induced fibrosarcoma. These tumors are usually rich in TAM, which are recruited at tumor sites primarily by the chemokine CCL2, produced by macrophages themselves and to a lower extent by tumor cells. Our group previously reported that TAM have essential trophic functions for fibrosarcoma cells, and their pharmacological depletion or inhibition of recruitment, significantly impair tumor growth. Furthermore, macrophages in tumors strongly correlate with higher metastatic ability [94, 95].

Based on our previous experience, it was therefore surprising to find fewer TAM in Osteoactivin-transduced tumors which grew faster, formed larger masses and were metastatic. When we explored the expression of CCL2 in tumors, this chemokine was significantly less produced, which may explain the low presence of macrophages. Although we cannot exclude that Osteoactivin directly inhibits the expression of CCL2, the most likely explanation is that the few macrophages inside OA-transduced tumors produce too little CCL2 to amplify the recruitment of blood circulating monocytes. The question, then, is why tumor cells have such a high proliferative rate even in the absence of the trophic effect of macrophages. Our subsequent results, as discussed below, point to an effect of Osteoactivin directly on cancer cells.

Other differences were apparent in the micro-environment of OA-transduced tumors. We observed a reduced number of blood vessels, which is also counter-intuitive in large tumor volumes, and lower levels of the vascular growth factor VEGF. Instead, a greater number of activated fibroblasts and increased collagen deposition were found compared to MOCK-transduced tumors. More collagen deposition is likely the result of more active fibroblasts which might be stimulated by the increased expression of FGF in these tumors. These results may be related to the described ability of Osteoactivin in promoting tissue healing in experimental models of tissue injury [75]. Along this line, also MMPs, such as MMP2, were increased in OA-positive tumors. In the literature, MMP2 expression has been regarded as a major determinant of the metastatic ability of Osteoactivin positive tumors [93]. Finally, we preliminarily investigated the infiltration of CD3+ lymphocytes in OA-transduced tumors and, although no definitive conclusions can be made, there were no substantial differences (not shown).

An important observation that shed light on the biological function of Osteoactivin in tumors was the different behavior of OA+ tumor cells and MOCK-cells in vitro. We found that when cultured *in vitro* in sub-optimal conditions (low nutrients, serum-free), OA+ tumor cells were able to survive for several days, while MOCK-cells rapidly died. OA-expressing cells progressively detached from plastic and formed large spheroids, growing in an anchoring-independent manner. These features are reminiscent of those displayed by cancer stem cells (CSC).

The existence of CSC or tumor-initiating cells has been confirmed in a variety of tumors, including breast, lung, colon, pancreatic and prostate cancer, as well as in melanoma, glioblastoma, hepatocellular carcinoma, and acute myeloid leukaemia [96-98]. CSC rest in a peculiar cellular niche within the tumor mass where they are protected from immuno-surveillance, apoptosis and chemotherapeutic drugs; the niche provides key signals that sustain, drive and promote their stemness [99, 100].

The connection between macrophages in tumors and CSC has been studied only in recent years [101]. It has been reported that TAM and CSC are subject to an intense cross-talk in which the production of TGFβ or growth factors (EGF) by TAM, supports CSC survival and protect them against external apoptotic signals; CSC, in turn, attract and reeducate macrophages through the secretion of chemoattractants, among which CCL2, CCL5 and VEGF-A, to eventually support tumor growth. TAM number and disposition in tumor niche seem to be correlated with number and disposition of CSC [102-105].

To confirm the hypothesis that OA-producing tumor cells might contain a higher proportion of CSC, we propagated spheroids in culture and observed that only OA-cells were able to form secondary and tertiary spheres, while MOCK cells did not have this self-renew ability. We next investigated the expression of various stem cell markers in our fibrosarcoma cells grown as spheroid and, indeed, the expression of Sox2, NANOG, OCT 3/4 and Brachyury was higher in OA-tumor cells forming spheres, compared to MOCK-tumors not producing Osteoactivin. Notably, the enrichment of stem cell markers was also confirmed in tumors samples grown *in vivo* from OA-tumor cells.

Furthermore, as an important feature of CSC is to be tumorigenic, we performed an in vivo experiment by injecting in mice only 1000 cells, a very low cell number. Osteoactivin-transduced fibrosarcoma cells were able to form tumors in just 15 days. Although also MOCK cells were tumorigenic, tumors were palpable much later, after 30 days.

Collectively, these results indicate that Osteoactivin has an important effect in promoting the survival, proliferation and stemness of tumor cells.

50

These findings open new questions that we need to address in the near future. An important issue is to reproduce these results with other tumor cell lines. We will first test another Osteoactivin-transduced fibrosarcoma (G3OA and G3Mock) and inject them in NSG mice to verify and obtain confirmation that OA-expressing tumor cells grow more rapidly in vivo. Furthermore, we have already screened several other tumor cell lines for their spontaneous ability to produce and secrete Osteoactivin; we will evaluate in vitro if Osteoactivin-producing cancer cells preferentially form spheres in culture and acquire a stem cell phenotype. As a complementary experiment, we will silence the production of Osteoactivin in OA-producing tumor cells and evaluate if tumor take and growth is decreased.

An important question is the role of macrophages that, we know, produce Osteoactivin when co-cultured with tumor cells. Is the macrophage-derived Osteoactivin able to sustain tumor proliferation and stemness? To explore this question we will perform co-culture experiments of macrophages and Osteoactivin-defective tumor cell lines to evaluate whether Osteoactivin produced by macrophages is able to up-regulate stem cell markers and induce sphere-forming ability in tumor cells.

Furthermore, to unequivocally identify the nature of the Osteoactivin-producing cells in the tumor micro-environment, we will perform a bone marrow transplant experiment (BM from DBA/2J Gpnmb$^+$ mice into DBA/2J mice). This experiment will allow us to demonstrate if hematopoietic cells (monocytes) recruited at tumor sites are the source of Osteoactivin, or instead, other stromal cells such as fibroblasts are the producer cells.

In conclusion, we have provided initial demonstration that a factor produced by macrophages in the tumor context facilitates the amplification of cells with CSC features, thus favoring tumor proliferation and dissemination and likely resistance to therapeutic strategies. This new pathway of Osteoactivin-mediated macrophage-cancer cell cross-talk adds on the already long list of pro-tumoral activities of TAM.

MATHERIALS AND METHODS

Cell biology

Cell culture

Human PT45 and PANC1 tumor cell lines, murine P815, MN-MCA1, PANC02, G2, G3, G4, G5, G2 OA and G2 MOCK tumor cell lines were cultured in RPMI1640 (Lonza) supplemented with 10% FBS (Sigma), 2mM L-glutamine, 100 U/mL penicillin and 100 μg/mL streptomycin (all from Life Technologies Inc.) and in tissue culture flasks (Corning, Stone Staffordshire, UK) at 37 °C and 5% CO_2.

In order to obtain spheroids from G2 OA and G2 MOCK cells we cultured them in Iscove medium (with 1%FBS or without FBS) and supplemented with specific factors: mEGF, mFGF (PeproTech), B27 and N2.

Cell stimulation and Tumor-Conditioned Media Preparation

Monocytes were stimulated with Glucocorticoids (MP Biomedicals) used 100uM; hM-CSF, GM-CSF, TGFβ, IL-10, IL-1, IL-13, IL-4, TNFα, INFγ, (Peprotech) used 25ng/ml; LPS (Alexis) 100ng/ml; Pam3Cys (Vinci Biochem) 2ug/ml according to the manufacture's instructions.

Tumor-conditioned media were prepared using Human PT45 and PANC1 tumor cell lines, murine P815, MN-MCA1, PANC02, MCA-1 and MCA-2 tumor cell lines following M&M described in Solinas et al 2010 [59].

Macrophage differentiation and polarization

Human monocytes were obtained from normal blood donor buffy coats by two-step gradient centrifugation. PBMCs were isolated by Histopaque-1077 density gradient centrifugation (SIGMA). Separation of monocyte and T cells was obtained from PBMCs by Percoll density

gradient centrifugation (GE Healthcare). Residual T and B cells were removed from monocyte fraction by plastic adherence in serum free RPMI . Murine BM-derived monocytes were obtained from femurs of 8-week-old male healthy mice and cultured O/N in RPMI 10%FBS. Non-adherent cells were plated in various culture conditions following the experimental plan as described below.

Macrophages and TC-Mφ were obtained by culturing 10^6/ml of human/murine monocytes for 6 days in RPMI 1640 5% FBS without other additions or supplemented with 25 ng/ml of human/murine recombinant M-CSF or in the presence of 30% of tumor cell line supernatants.

To obtain M1/M2 polarization we stimulated overnight M-CSF-differentiated macrophages with LPS (100 ng/ml) (PeproTech) and human/murine IFNγ (500 U/ml) (PeproTech) to obtain M1-Mf and with human/murine IL-4 (20 ng/ml) (PeproTech) to obtain M2-Mf. All samples were collected under endotoxin-free conditions.

Molecular biology

Real-time RT-PCR

Total RNA extraction from our samples was performed with pureZOL RNA isolation reagent (BIORAD). cDNA was synthesized by random priming from 2μg of total RNA with GeneAmp RNA PCR kit (Applied Biosystems), according to the manufacturer's instructions. Real-Time PCR was performed using SYBR Green dye and 7900HT Fast Real Time PCR Systems (Applied Biosystems). The sequences of primer pairs specific for each gene (Invitrogen) were designed with Primer Express Software (Applied Biosystems). Experiments were performed in triplicate for each sample. mRNA was normalized to GAPDH mRNA by subtracting the cycle threshold (Ct) value of GAPDH mRNA from the Ct value of the gene (ΔCt). Fold difference (2^-ΔΔCt) was calculated by comparing ΔCt values.

Protein detection by Elisa

To determine the production of human/murine Osteoactivin , tumor cell lines/macrophages supernatants were collected, centrifuged, filtered and stored at -20°. Proteins levels were measured by commercially available human/murine ELISA kits, according to the manufacture's instructions (R&D Systems). Data were analyzed with SoftMax Pro 5.3 software.

Bio-plex Protein Array system

IL1β, IL10, IL17, IL13, CCL2, CCL3, CCL4, Eotaxin, TNFα, were measured in duplicate into monocytes/macrophages supernatants using the Bio-plex Protein Array system (BioRad), according to the manufacturer instructions. Our assay (Bio-plex Pro Muose Cytokine Standard 23-plex, groupI) was customized to detect and quantify for each cytokine, eight standard points ranged from 2.00 to 40.000 pg/ml and the minimum detectable dose was <10pg/ml.

Data from the reaction are acquired using the Bio-Plex system, analysed and presented as fluorescence intensity (FI) and target concentration on Bio-Plex Manager software.

Osteoactivin cell transduction

To assess Osteoactivin functions *in vitro* we generated tumor cell lines stably over-expressing OA. We transduced MCA-OA- cell lines G2 and G3 with a lentiviral plasmid that allows to constitutively express endogenous OA. For this reason we exploited a plasmid previously generated in the laboratory in which the murine coding sequence of *Gpnmb* was cloned in frame with the fluorescent reporter mCherry under the CMV promoter in a lentiviral vector called OA-mCherry pRRL-Sin, and as a control the empty vector containing only mCherry, named mCherry pRRL-Sin. Transduction of G2 and G3 MCA cell lines was performed generating viral particles with HEK293T cells transfected with Lipofectamine2000 (ThermoFisher Scientific) according to manufacturer's instruction. Briefly, cells transfected with a ratio of 2:1:2 of packaging plasmid (pCMV-Delta 8.2), envelope plasmid (pVSV-G) and tranfer plasmid (mCherry pRRL-Sin or OA-

mCherry pRRL-Sin) respectively, and after 24 hours the media was replaced. 48 hours after transfection, the replaced media containing viral particles was collected, centrifuged to pellet HEK293T cells, filtered through a 0,45μm-sized filter, and used to replace the media of 50% confluent MCA cell lines, while fresh media was added to transfected HEK293T cells to do repeat the transduction procedure. Cell lines generated were expanded 24 hours after the last transduction to assess Osteoactivin expression by flow cytometry and ELISA as described.

In vitro functional tests

Cell adhesion assay

Plates were coated with 2ug/ml of recombinant human Osteoactivin or serum free RPMI (coating control) for 2 hrs at 37 °C and washed two times. Cells were then plated for adherence at 37 °C for 90 minutes. Non-adherent cells were removed by carefully washing plates while adherent cells were fixed and stained with Diff-Quik (Medion Diagnostics*)* according to the manufacture's instructions. Diff-Quik was rinsed out of the wells with water, and the plates were allowed to dry. Stained cells were counted considering 5 different areas.

Cell migration assay

Cell migration was evaluated using transwell system with 5 μm pore size in 24 well plate (Costar). 10^5 cells were suspended in 200ul of medium and plated onto the membrane in the upper chamber; the lower chamber was filled with 600 ul of medium containing different concentrations (50-100 ug/ml) of recombinant OA (R&D). RPMI 1%FBS or recombinant CCL2 (100 ug/ml) were used respectively as negative and positive control. After 90 minutes of incubation we counted migrated cells contained into the lower chamber.

Flow cytometry

To measure the expression of cell surface molecules, cells were were blocked using PBS 1% human/mouse serum and routinely stained and analyzed by flow cytometry on FACS Canto (BD Bioscience). For staining procedures, cells were washed and resuspended in FACS buffer.

To analyzed the expression of stemness marker we used: PerCp-Rat CD45, Ecadherin- PE, B-catenin FITC, CD47 APC, CD49b PE, CD 49e PE, CD61 FITC, CD41 BV450, CD51 PE, CD54 Pacif Blue, CD34 FITC, CD117 PECy7, Sca1 PECy7, CD44 FITC, CD135 PE, RANK PE, CD138 APC, CD71 FITC (BD Bioscience); Anti-mouse PE F4/80 (AbD Serotec); Pacific Blue-Rat CD11b (Biolegend). Labeled cells were fixed in PBS-/- 1X 1% formalin. After staining procedures, acquisition was performed by FACS CantoII instrument (BD Biosciences) and analyzed by FACS Diva and FlowJo software version 6.1.1 (BD Biosciences). For SOX2 (ThermoFisher) intracellular staining we used the BD Fixation/Permeabilization solution kit and Perm-wash to wash samples between various steps of the staining. Flow cytometry analysis was performed by FACS CantoTM instrument and FACS Diva software version 6.1.1 (BD Biosciences).

Mouse tumor models

Mice were used in compliance with national (4D.L.N.116, G.U., suppl. 40, 18-2-1992) and international law and policies (EEC Council Directive 86/609, OJ L 358, 1, 12-12-1987; NIH Guide for the Care and Use of Laboratory Animals, US National Research Council 1996). DBA/2J Gpnmb$^+$ were purchased from the Jackson Laboratory (Bar Harbor, ME) and maintained and breaded at Charles River (Calco, Milano); DBA/2J mice of 8 weeks were directly purchased from Charles River. Tumors were induced by intraperitoneal or intramuscular injection of tumour cells; the number of injected cells is variable depending on the type of experiment.

Immunohistochemistry and immunofluorescence

Paraffin embedded Murine tissues were cut at 3 um and put on superfrost slides. After dewaxing and rehydration, antigen unmasking were performed in decloaking chamber in DIVA buffer (Biocare Medical) and with citrate buffer pH 6.00 in thermostatic bath (for Ki67). Endogenous peroxidases were blocked with 2% H_2O_2 for 20 minutes and then rodent block M were used to block unspecific binding sites. Sections were incubated with rat anti mouse CD68 1:100 (clone FA-11 Hycult Biotechnology), rat anti mouse F4/80 1:400 (AbD Serotec), goat anti mouse CD31 1:1000 (R&D Systems), rabbit anti mouse αSMA 1:300 (Biocare Medical) and rabbit anti mouse Ki67 1:400 (Cell Signaling). All the primary antibodies were incubated for 1 hour in humid chamber. As secondary antibody we used Rat on Mouse HRP polymer kit (Biocare Medical) for CD68 and F4/80, Goat on rodent HRP (Biocare Medical) for CD31 and MACH 1 Universal HRP-Polymer Detection (Biocare Medical) for αSMA and Ki67. Reactions were developed with 3,3'-Diaminobenzidine, DAB, (Biocare Medical), than counterstained with hematoxylin and mounted with Eukitt.

For collagen, sections were cut at 3 um, put on non-polarized slides and after dewaxing and rehydration, Sirius red staining was performed.

In each experiment 5-8 tumors/group were analyzed, results are the mean of immunoreactive areas in 4 slices for tumor. For CD31 results are expressed as mean of number of positive vessels per areas in 4 slices for tumor. The analyses were performed with Image Pro-Analyzer 7.0 (Media Cybernetics) on pictures at the same magnifications.

Statistical analysis

Statistical analysis was performed using a paired or unpaired Student's t-test. P-values of less than 0.05 were considered significant.

BIBLIOGRAPHY

1. Klemparskaya, N.N., *100 years of the phagocytosis doctrine (Ilya Ilyich Mechnikov).* J Hyg Epidemiol Microbiol Immunol, 1983. **27**(3): p. 249-52.
2. Gordon, S., A. Plüddemann, and F. Martinez Estrada, *Macrophage heterogeneity in tissues: phenotypic diversity and functions.* Immunol Rev, 2014. **262**(1): p. 36-55.
3. Geissmann, F., et al., *Development of Monocytes, Macrophages, and Dendritic Cells.* Science, 2010. **327**(5966): p. 656-661.
4. Ginhoux, F., et al., *New insights into the multidimensional concept of macrophage ontogeny, activation and function.* Nature Immunology, 2015. **17**(1): p. 34-40.
5. Gordon, S. and P.R. Taylor, *Monocyte and macrophage heterogeneity.* Nature Reviews Immunology, 2005. **5**(12): p. 953-964.
6. Wynn, T.A., A. Chawla, and J.W. Pollard, *Macrophage biology in development, homeostasis and disease.* Nature, 2013. **496**(7446): p. 445-455.
7. Mantovani, A., et al., *The chemokine system in diverse forms of macrophage activation and polarization.* Trends Immunol, 2004. **25**(12): p. 677-86.
8. Mantovani, A., et al., *The chemokine system in cancer biology and therapy.* Cytokine & Growth Factor Reviews, 2010. **21**(1): p. 27-39.
9. Wermuth, P.J. and S.A. Jimenez, *The significance of macrophage polarization subtypes for animal models of tissue fibrosis and human fibrotic diseases.* Clinical and Translational Medicine, 2015. **4**(1).
10. Sica, A. and A. Mantovani, *Macrophage plasticity and polarization: in vivo veritas.* Journal of Clinical Investigation, 2012. **122**(3): p. 787-795.
11. Allavena, P. and A. Mantovani, *Immunology in the clinic review series; focus on cancer: tumour-associated macrophages: undisputed stars of the inflammatory tumour microenvironment.* Clinical & Experimental Immunology, 2012. **167**(2): p. 195-205.
12. Murray, Peter J., et al., *Macrophage Activation and Polarization: Nomenclature and Experimental Guidelines.* Immunity, 2014. **41**(1): p. 14-20.
13. Solinas, G., et al., *Tumor-associated macrophages (TAM) as major players of the cancer-related inflammation.* J Leukoc Biol, 2009. **86**(5): p. 1065-1073.
14. Lawrence, T. and G. Natoli, *Transcriptional regulation of macrophage polarization: enabling diversity with identity.* Nature Reviews Immunology, 2011. **11**(11): p. 750-761.
15. Xue, J., et al., *Transcriptome-Based Network Analysis Reveals a Spectrum Model of Human Macrophage Activation.* Immunity, 2014. **40**(2): p. 274-288.
16. Mantovani, A., et al., *Cancer-related inflammation.* Nature, 2008. **454**(7203): p. 436-444.
17. Hanahan, D. and Robert A. Weinberg, *Hallmarks of Cancer: The Next Generation.* Cell, 2011. **144**(5): p. 646-674.
18. Noy, R. and Jeffrey W. Pollard, *Tumor-Associated Macrophages: From Mechanisms to Therapy.* Immunity, 2014. **41**(1): p. 49-61.
19. Bottazzi, B., et al., *Regulation of the macrophage content of neoplasms by chemoattractants.* Science, 1983. **220**(4593): p. 210-212.
20. Qian, B.-Z., et al., *CCL2 recruits inflammatory monocytes to facilitate breast-tumour metastasis.* Nature, 2011. **475**(7355): p. 222-225.
21. Balkwill, F., *Cancer and the chemokine network.* Nature Reviews Cancer, 2004. **4**(7): p. 540-550.
22. Bingle, L., N.J. Brown, and C.E. Lewis, *The role of tumour-associated macrophages in tumour progression: implications for new anticancer therapies.* The Journal of Pathology, 2002. **196**(3): p. 254-265.
23. Mantovani, A. and P. Allavena, *The interaction of anticancer therapies with tumor-associated macrophages.* J Exp Med, 2015. **212**(4): p. 435-445.

24. Tang, X., *Tumor-associated macrophages as potential diagnostic and prognostic biomarkers in breast cancer.* Cancer Lett, 2013. **332**(1): p. 3-10.

25. Jung, K.Y., et al., *Cancers with Higher Density of Tumor-Associated Macrophages Were Associated with Poor Survival Rates.* Journal of Pathology and Translational Medicine, 2015. **49**(4): p. 318-324.

26. Lee, Y. and S.K. Biswas, *Rewiring macrophages for anti-tumour immunity.* Nat Cell Biol, 2016. **18**(7): p. 718-720.

27. Sainz, B., Jr., et al., *Cancer Stem Cells and Macrophages: Implications in Tumor Biology and Therapeutic Strategies.* Mediators Inflamm, 2016. **2016**: p. 9012369.

28. Dvorak, H.F., et al., *Tumor microenvironment and progression.* J Surg Oncol, 2011. **103**(6): p. 468-74.

29. Schiavoni, G., L. Gabriele, and F. Mattei, *The tumor microenvironment: a pitch for multiple players.* Front Oncol, 2013. **3**: p. 90.

30. Turley, S.J., V. Cremasco, and J.L. Astarita, *Immunological hallmarks of stromal cells in the tumour microenvironment.* Nat Rev Immunol, 2015. **15**(11): p. 669-82.

31. Adams, J.C., *Cell-matrix contact structures.* Cell Mol Life Sci, 2001. **58**(3): p. 371-92.

32. Brodt, P., *Role of the microenvironment in liver metastasis: from pre- to pro-metastatic niches.* Clinical Cancer Research, 2016.

33. Goddard, E.T., et al., *Quantitative extracellular matrix proteomics to study mammary and liver tissue microenvironments.* The International Journal of Biochemistry & Cell Biology, 2016.

34. Cox, T.R. and J.T. Erler, *Remodeling and homeostasis of the extracellular matrix: implications for fibrotic diseases and cancer.* Dis Model Mech, 2011. **4**(2): p. 165-78.

35. Frantz, C., K.M. Stewart, and V.M. Weaver, *The extracellular matrix at a glance.* J Cell Sci, 2010. **123**(Pt 24): p. 4195-200.

36. Huijbers, I.J., et al., *A role for fibrillar collagen deposition and the collagen internalization receptor endo180 in glioma invasion.* PLoS One, 2010. **5**(3): p. e9808.

37. Jussila, T., et al., *Synthesis and maturation of type I and type III collagens in endometrial adenocarcinoma.* Eur J Obstet Gynecol Reprod Biol, 2004. **115**(1): p. 66-74.

38. Siegwart, J.T., Jr. and T.T. Norton, *Selective regulation of MMP and TIMP mRNA levels in tree shrew sclera during minus lens compensation and recovery.* Invest Ophthalmol Vis Sci, 2005. **46**(10): p. 3484-92.

39. Sawaguchi, N., et al., *Extracellular matrix modulates expression of cell-surface proteoglycan genes in fibroblasts.* Connect Tissue Res, 2006. **47**(3): p. 141-8.

40. Bourguignon, L.Y., M. Shiina, and J.J. Li, *Hyaluronan-CD44 interaction promotes oncogenic signaling, microRNA functions, chemoresistance, and radiation resistance in cancer stem cells leading to tumor progression.* Adv Cancer Res, 2014. **123**: p. 255-75.

41. Nasser, N.J., *Heparanase involvement in physiology and disease.* Cell Mol Life Sci, 2008. **65**(11): p. 1706-15.

42. Sorokin, L., *The impact of the extracellular matrix on inflammation.* Nat Rev Immunol, 2010. **10**(10): p. 712-23.

43. Sorokin, L., *The impact of the extracellular matrix on inflammation.* Nature Reviews Immunology, 2010. **10**(10): p. 712-723.

44. Insua-Rodríguez, J. and T. Oskarsson, *The extracellular matrix in breast cancer.* Advanced Drug Delivery Reviews, 2016. **97**: p. 41-55.

45. Mott, J.D. and Z. Werb, *Regulation of matrix biology by matrix metalloproteinases.* Curr Opin Cell Biol, 2004. **16**(5): p. 558-64.

46. Afik, R., et al., *Tumor macrophages are pivotal constructors of tumor collagenous matrix.* J Exp Med, 2016. **213**(11): p. 2315-2331.

47. Liguori, M., et al., *Tumor-Associated Macrophages as Incessant Builders and Destroyers of the Cancer Stroma.* Cancers (Basel), 2011. **3**(4): p. 3740-3761.

48. Zollinger, A.J. and M.L. Smith, *Fibronectin, the extracellular glue.* Matrix Biology, 2016.

49. Stenina-Adognravi, O., *Thrombospondins.* Current Opinion in Lipidology, 2013. **24**(5): p. 401-409.

50. Rangaswami, H., A. Bulbule, and G.C. Kundu, *Osteopontin: role in cell signaling and cancer progression.* Trends in Cell Biology, 2006. **16**(2): p. 79-87.

51. Kara A. Furger, B.S.P., et al., *The Functional and Clinical Roles of Osteopontin in Cancer and Metastasis.* Current Molecular Medicine, 2001. **1**(5): p. 621-632.

52. Bradshaw, A.D. and E.H. Sage, *SPARC, a matricellular protein that functions in cellular differentiation and tissue response to injury.* Journal of Clinical Investigation, 2001. **107**(9): p. 1049-1054.

53. Balkwill, F. and A. Mantovani, *Inflammation and cancer: back to Virchow?* The Lancet, 2001. **357**(9255): p. 539-545.

54. Esquivel-Velázquez, M., et al., *The Role of Cytokines in Breast Cancer Development and Progression.* Journal of Interferon & Cytokine Research, 2015. **35**(1): p. 1-16.

55. Emilie, D., et al., *Intratumoral Production of IL-6 in B Cell Chronic Lymphocytic Leukemia and B Lymphomas.* Leukemia & Lymphoma, 2009. **11**(5-6): p. 411-417.

56. Flavell, R.A., et al., *The polarization of immune cells in the tumour environment by TGFβ.* Nature Reviews Immunology, 2010. **10**(8): p. 554-567.

57. Goel, H.L. and A.M. Mercurio, *VEGF targets the tumour cell.* Nature Reviews Cancer, 2013. **13**(12): p. 871-882.

58. Mannino, M.H., et al., *The paradoxical role of IL-10 in immunity and cancer.* Cancer Lett, 2015. **367**(2): p. 103-107.

59. Solinas, G., et al., *Tumor-conditioned macrophages secrete migration-stimulating factor: a new marker for M2-polarization, influencing tumor cell motility.* J Immunol, 2010. **185**(1): p. 642-52.

60. Maric, G., et al., *Glycoprotein non-metastatic b (GPNMB): A metastatic mediator and emerging therapeutic target in cancer.* Onco Targets Ther, 2013. **6**: p. 839-52.

61. Selim, A.A., *Osteoactivin bioinformatic analysis: prediction of novel functions, structural features, and modes of action.* Med Sci Monit, 2009. **15**(2): p. MT19-33.

62. Rose, A.A., et al., *ADAM10 releases a soluble form of the GPNMB/Osteoactivin extracellular domain with angiogenic properties.* PLoS One, 2010. **5**(8): p. e12093.

63. Shikano, S., et al., *Molecular Cloning of a Dendritic Cell-associated Transmembrane Protein, DC-HIL, That Promotes RGD-dependent Adhesion of Endothelial Cells through Recognition of Heparan Sulfate Proteoglycans.* Journal of Biological Chemistry, 2000. **276**(11): p. 8125-8134.

64. Chung, J.S., et al., *The DC-HIL/syndecan-4 pathway regulates autoimmune responses through myeloid-derived suppressor cells.* J Immunol, 2014. **192**(6): p. 2576-84.

65. Ripoll, V.M., et al., *Gpnmb is induced in macrophages by IFN-gamma and lipopolysaccharide and acts as a feedback regulator of proinflammatory responses.* J Immunol, 2007. **178**(10): p. 6557-66.

66. Gabriel, T.L., et al., *Lysosomal stress in obese adipose tissue macrophages contributes to MITF-dependent Gpnmb induction.* Diabetes, 2014. **63**(10): p. 3310-23.

67. Ripoll, V.M., et al., *Microphthalmia transcription factor regulates the expression of the novel osteoclast factor GPNMB.* Gene, 2008. **413**(1-2): p. 32-41.

68. Abe, H., et al., *Transgenic expression of osteoactivin in the liver attenuates hepatic fibrosis in rats.* Biochem Biophys Res Commun, 2007. **356**(3): p. 610-5.

69. Abdelmagid, S.M., et al., *Osteoactivin, an anabolic factor that regulates osteoblast differentiation and function.* Exp Cell Res, 2008. **314**(13): p. 2334-51.

70.   Anderson, M.G., et al., *Mutations in genes encoding melanosomal proteins cause pigmentary glaucoma in DBA/2J mice.* Nat Genet, 2002. **30**(1): p. 81-85.

71.   Chang, B., et al., *Interacting loci cause severe iris atrophy and glaucoma in DBA/2J mice.* Nat Genet, 1999. **21**(4): p. 405-9.

72.   Rose, A.A. and P.M. Siegel, *Emerging therapeutic targets in breast cancer bone metastasis.* Future Oncol, 2010. **6**(1): p. 55-74.

73.   Rose, A.A., et al., *Glycoprotein nonmetastatic B is an independent prognostic indicator of recurrence and a novel therapeutic target in breast cancer.* Clin Cancer Res, 2010. **16**(7): p. 2147-56.

74.   Furochi, H., et al., *Osteoactivin fragments produced by ectodomain shedding induce MMP-3 expression via ERK pathway in mouse NIH-3T3 fibroblasts.* FEBS Lett, 2007. **581**(30): p. 5743-50.

75.   Li, B., et al., *The melanoma-associated transmembrane glycoprotein Gpnmb controls trafficking of cellular debris for degradation and is essential for tissue repair.* FASEB J, 2010. **24**(12): p. 4767-81.

76.   Abdelmagid, S.M., et al., *Temporal and spatial expression of osteoactivin during fracture repair.* J Cell Biochem, 2010. **111**(2): p. 295-309.

77.   Ogawa, T., et al., *Osteoactivin upregulates expression of MMP-3 and MMP-9 in fibroblasts infiltrated into denervated skeletal muscle in mice.* Am J Physiol Cell Physiol, 2005. **289**(3): p. C697-707.

78.   Pahl, M.V., et al., *Upregulation of monocyte/macrophage HGFIN (Gpnmb/Osteoactivin) expression in end-stage renal disease.* Clin J Am Soc Nephrol, 2010. **5**(1): p. 56-61.

79.   Tomihari, M., et al., *Gpnmb is a melanosome-associated glycoprotein that contributes to melanocyte/keratinocyte adhesion in a RGD-dependent fashion.* Experimental Dermatology, 2009. **18**(7): p. 586-595.

80.   Moussa, F.M., et al., *Osteoactivin Promotes Osteoblast Adhesion Through HSPG and αvβ1 Integrin.* J Cell Biochem, 2014. **115**(7): p. 1243-1253.

81.   Cook, D.N., *Spontaneous Mutations in Recombinant Inbred Mice: Mutant Toll-like Receptor 4 (Tlr4) in BXD29 Mice.* Genetics, 2005. **172**(3): p. 1751-1755.

82.   Wells, C.A., et al., BMC Immunology, 2003. **4**(1): p. 5.

83.   Germano, G., et al., *Role of Macrophage Targeting in the Antitumor Activity of Trabectedin.* Cancer Cell, 2013. **23**(2): p. 249-262.

84.   Chung, J.S., et al., *Binding of DC-HIL to Dermatophytic Fungi Induces Tyrosine Phosphorylation and Potentiates Antigen Presenting Cell Function.* The Journal of Immunology, 2009. **183**(8): p. 5190-5198.

85.   Tsui, K.-H., et al., *Glycoprotein transmembrane nmb: An androgen-downregulated gene attenuates cell invasion and tumorigenesis in prostate carcinoma cells.* The Prostate, 2012. **72**(13): p. 1431-1442.

86.   Fiorentini, C., et al., *GPNMB/OA protein increases the invasiveness of human metastatic prostate cancer cell lines DU145 and PC3 through MMP-2 and MMP-9 activity.* Exp Cell Res, 2014. **323**(1): p. 100-111.

87.   Chung, J.-S., et al., *DC-HIL-Expressing Myelomonocytic Cells Are Critical Promoters of Melanoma Growth.* Journal of Investigative Dermatology, 2014. **134**(11): p. 2784-2794.

88.   Tse, K.F., *CR011, a Fully Human Monoclonal Antibody-Auristatin E Conjugate, for the Treatment of Melanoma.* Clinical Cancer Research, 2006. **12**(4): p. 1373-1382.

89.   Sondag, G.R., et al., *Osteoactivin inhibition of osteoclastogenesis is mediated through CD44-ERK signaling.* Experimental & Molecular Medicine, 2016. **48**(9): p. e257.

90.   Wells, C.A., et al., *Genetic control of the innate immune response.* BMC Immunology, 2003. **4**(1): p. 5.

91.   Chella Krishnan, K., et al., *Host Genetic Variations and Sex Differences Potentiate Predisposition, Severity, and Outcomes of Group A Streptococcus-Mediated Necrotizing Soft Tissue Infections.* Infection and Immunity, 2016. **84**(2): p. 416-424.

92.   Dengler, L., et al., *Immunization with live virus vaccine protects highly susceptible DBA/2J mice from lethal influenza A H1N1 infection.* Virology Journal, 2012. **9**(1): p. 212.

93.   Rose, A.A.N., et al., *Osteoactivin Promotes Breast Cancer Metastasis to Bone.* Molecular Cancer Research, 2007. **5**(10): p. 1001-1014.

94.   Germano, G., et al., *Role of macrophage targeting in the antitumor activity of trabectedin.* Cancer Cell, 2013. **23**(2): p. 249-62.

95.   Biswas, S.K., *A distinct and unique transcriptional program expressed by tumor-associated macrophages (defective NF- B and enhanced IRF-3/STAT1 activation).* Blood, 2006. **107**(5): p. 2112-2122.

96.   Li, C., et al., *Identification of pancreatic cancer stem cells.* Cancer Res, 2007. **67**(3): p. 1030-7.

97.   Hermann, P.C., et al., *Distinct populations of cancer stem cells determine tumor growth and metastatic activity in human pancreatic cancer.* Cell Stem Cell, 2007. **1**(3): p. 313-23.

98.   Al-Hajj, M., et al., *Prospective identification of tumorigenic breast cancer cells.* Proc Natl Acad Sci U S A, 2003. **100**(7): p. 3983-8.

99.   Hsu, Y.C. and E. Fuchs, *A family business: stem cell progeny join the niche to regulate homeostasis.* Nat Rev Mol Cell Biol, 2012. **13**(2): p. 103-14.

100.   Plaks, V., N. Kong, and Z. Werb, *The cancer stem cell niche: how essential is the niche in regulating stemness of tumor cells?* Cell Stem Cell, 2015. **16**(3): p. 225-38.

101.   Fan, Q.M., et al., *Tumor-associated macrophages promote cancer stem cell-like properties via transforming growth factor-beta1-induced epithelial-mesenchymal transition in hepatocellular carcinoma.* Cancer Lett, 2014. **352**(2): p. 160-8.

102.   Zeppernick, F., et al., *Stem cell marker CD133 affects clinical outcome in glioma patients.* Clin Cancer Res, 2008. **14**(1): p. 123-9.

103.   Pallini, R., et al., *Cancer stem cell analysis and clinical outcome in patients with glioblastoma multiforme.* Clin Cancer Res, 2008. **14**(24): p. 8205-12.

104.   Jinushi, M., et al., *Tumor-associated macrophages regulate tumorigenicity and anticancer drug responses of cancer stem/initiating cells.* Proceedings of the National Academy of Sciences, 2011. **108**(30): p. 12425-12430.

105.   Mitchem, J.B., et al., *Targeting Tumor-Infiltrating Macrophages Decreases Tumor-Initiating Cells, Relieves Immunosuppression, and Improves Chemotherapeutic Responses.* Cancer Res, 2012. **73**(3): p. 1128-1141.